

1 **The dynamic of the annual carbon allocation to wood in**
2 **European tree species is consistent with a combined source-**
3 **sink limitation of growth: implications for modelling**

4

5 **J. Guillemot¹, N. K. Martin-StPaul^{1,2}, E. Dufrêne¹, C. François¹, K. Soudani¹, J. M.**
6 **Ourcival³ and N. Delpierre¹**

7 [1]{Laboratoire Ecologie, Systématique et Evolution, Université Paris Sud, CNRS,
8 AgroParisTech, UMR8079, F-91405 Orsay, France }

9 [2]{Ecologie des Forêts Méditerranéennes, INRA, UR629, F-84914 Avignon, France }

10 [3]{CEFE, CNRS, Université de Montpellier, Université Paul-Valéry Montpellier, EPHE,
11 UMR5175, F-34293 Montpellier, France }

12 Correspondence to: J. Guillemot (joannes.guillemot@gmail.com)

13

14

15

16 **Abstract**

17 The extent to which wood growth is limited by carbon (C) supply (i.e., source control) or by
18 cambial activity (i.e., sink control) will strongly determine the responses of trees to global
19 changes. Nevertheless, the physiological processes that are responsible for limiting forest growth
20 are still debated. The aim of this study was to evaluate the key determinants of the annual C
21 allocation to wood along large soil and climate regional gradients over France. The study was
22 conducted for five tree species representative of the main European forest biomes (*Fagus*
23 *sylvatica*, *Quercus petraea*, *Quercus ilex*, *Quercus robur* and *Picea abies*).

24 The drivers of stand biomass growth were assessed on both inter-site and inter-annual scales. Our
25 dataset comprised field measurements performed at 49 sites (931 site-years) that included
26 biometric measurements and a variety of stand characteristics (e.g., soil water holding capacity,
27 leaf area index). It was complemented with process-based simulations when possible explanatory
28 variables could not be directly measured (e.g., annual and seasonal tree C balance, bioclimatic
29 water stress indices). Specifically, the relative influences of tree C balance (source control), direct
30 environmental control (water and temperature controls of sink activity) and allocation
31 adjustments related to age, past climate conditions, competition intensity and soil nutrient
32 availability on growth were quantified.

33 The inter-site variability in the stand C allocation to wood was predominantly driven by age-
34 related decline. The direct effects of temperature and water stress on sink activity (i.e., effects
35 independent from their effects on the C supply) exerted a strong influence on the annual stand
36 wood growth in all of the species considered, including deciduous temperate species. The lagged
37 effect of the past environmental conditions (e.g., the previous year's water stress and low C
38 uptake) significantly affected the annual C allocation to wood. The C supply appeared to strongly
39 limit growth only in temperate deciduous species.

40 We provide an evaluation of the spatio-temporal dynamics of the annual C allocation to wood in
41 French forests. Our study supports the premise that the growth of European tree species is subject
42 to complex control processes that include both source and sink limitations. The relative
43 influences of the growth drivers strongly vary with time and across spatial ecological gradients.
44 We suggest a straightforward modelling framework with which to implement these combined
45 forest growth limitations into terrestrial biosphere models.

46

47

48

49

50

51 **1 Introduction**

52 Forests play a critical role in the global carbon (C) cycle. Inventory-based estimates indicate that
53 established forests have been a persistent carbon sink for decades, sequestering almost 30% of the
54 world's total anthropogenic C emissions between 1990 and 2007 (Pan et al., 2011). The fate of
55 the sequestered C is highly dependent on the C dynamic in trees, which determines the residence
56 time of C in forest ecosystems. Despite its importance for the future terrestrial C sink (Carvalhais
57 et al., 2014; Friend et al., 2013), the partitioning of C among tree organs and ecosystem
58 respiration remains poorly understood (Brüggemann et al., 2011). In particular, there has been
59 considerable amount of debate regarding the physiological mechanisms that drive the increment
60 of the forest woody biomass (Palacio et al., 2014; Wiley and Helliker, 2012). The fraction of
61 assimilated C stored in woody biomass can be inferred by combining biometric measurements
62 with estimates of the C exchange between the ecosystem and atmosphere, based on the eddy-
63 covariance (EC) technique (Babst et al., 2014; Litton et al., 2007; Wolf et al., 2011). Global
64 meta-analyses (that included data from various biomes and species) have revealed a strong
65 correlation between the observed gross primary production (GPP) and the woody biomass
66 increment (Litton et al., 2007; Zha et al., 2013). Accordingly, growth has long been thought to be
67 C limited, because of the hypothesized causal link between C supply and growth (i.e., source
68 control, Sala *et al.* 2012). The environmental factors that have been reported to affect growth
69 (soil water content, temperature, nutrient content, light and CO₂) were therefore supposed to
70 operate through their effects on photosynthesis and respiration fluxes. This C-centric paradigm
71 underlies most of the C allocation rules formalized in the terrestrial biosphere models (TBMs)
72 that are currently used to evaluate the effects of global changes on forests (Clark et al., 2011;
73 Dufrêne et al., 2005; De Kauwe et al., 2014; Krinner et al., 2005; Sitch et al., 2003).

74 Source control of wood growth is a mechanism that has been questioned by several
75 authors, who argue that cambial activity is more sensitive than C assimilation to several
76 environmental stressors (Fatichi et al., 2014). In particular, the decrease in cell turgor that occurs
77 because of water stress strongly affects cell division and expansion (Woodruff and Meinzer,
78 2011) before there is any strong reduction in the gas exchange (Muller et al., 2011; Tardieu et al.,
79 2011). Similarly, cell division is affected by low temperatures before it is affected by
80 photosynthesis (Körner, 2008). The onset of cambial activity is also known to be highly

81 responsive to temperature (Delpierre et al., 2015; Kudo et al., 2014; Lempereur et al., 2015; Rossi
82 et al., 2011) and, in turn, may partly determine annual cell production and wood growth (Lupi et
83 al., 2010; Rossi et al., 2013). Finally, the quality and quantity of available soil nutrients,
84 particularly nitrogen (N), could affect growth independently of their impacts on C assimilation,
85 because of the relatively constrained stoichiometry of tree biomass (Leuzinger and
86 Hättenschwiler, 2013). These studies suggest that growth is limited by the direct effects of
87 environmental factors (i.e., sink control). However, numerous key environmental factors (e.g.,
88 nutrients, temperature and water) affect both sink and source activities, and it is thus difficult to
89 determine whether wood growth is more related to C supply or to the intrinsic environmental
90 sensitivity of cambium functioning (Fatichi et al., 2014). The extent to which wood growth is
91 under source or sink control is of paramount importance for predicting how trees will respond to
92 global changes and specifically how increasing atmospheric CO₂ will affect forest productivity
93 and the future terrestrial C sink. The implementation of the respective roles of source and sink
94 controls on growth in TBMs is therefore a substantial challenge for modellers, because it may
95 determine our ability to project future forest C sink, diebacks and distributions (Cheaib et al.,
96 2012; Fatichi et al., 2014; Leuzinger et al., 2013).

97 The allocation of assimilated C within forest ecosystems is a complex, integrative process
98 that can be described by several non-exclusive principles (Franklin et al., 2012) that include i)
99 allometric scaling, ii) functional balance and iii) evolution-based optimal responses. i) The
100 allometric scaling principle is based on the assumption that biophysical laws, such as the
101 mechanical constraints associated with plant hydraulic architecture and the construction of water-
102 transport system (Magnani et al., 2000), determine C partitioning among the different tree
103 compartments. ii) The functional balance principle suggests that the organ responsible for
104 acquiring the limiting resource is preferentially allocated C. Consistent with this principle, higher
105 C allocation to fine roots at the expense of C allocation to wood growth has been reported for
106 poor or dry soils (Chen et al., 2013; Keyes and Grier, 1981). In addition, a possibly greater
107 allocation to root symbionts and exudates at the expense of biomass production has also been
108 reported (Vicca et al., 2012). iii) Finally, the optimal response principle postulates that allocation
109 maximizes fitness in a fixed environment. This hypothesis agrees with the idea that a dynamic
110 reserve pool act as temporary storage, possibly at the expense of growth, to promote long-term
111 tree survival (Chapin et al., 1990; Sala et al., 2012). Indeed, time lags between C uptake and

112 growth have been reported (Gough et al., 2009; Richardson et al., 2013). The optimal response
113 principle is consistent with several well-known life history traits, such as preferential allocation
114 to reproduction in ageing plants, which could lead to age-related declines in woody biomass
115 allocation (Genet et al., 2010; Thomas, 2011). The woody biomass increment therefore appears to
116 be under the control of multiple factors. The effects of these drivers are expected to strongly vary
117 in space and time. Consequently, studies have reported conflicting relationships between the C
118 supply and wood growth (Gielen et al., 2013; Richardson et al., 2013), ranging from no
119 significant relationships (Mund et al., 2010; Rocha et al., 2006) to close relationships on seasonal
120 (Babst et al., 2014; Granier et al., 2008; Zweifel et al., 2010) or annual (Ohtsuka et al., 2009;
121 Peichl et al., 2010; Zweifel et al., 2010) time scales. Determining the key processes that affect
122 wood growth on different spatio-temporal scales is necessary to explain these apparently
123 contradictory results using a common framework. Moreover, investigations should be conducted
124 at the species level, because phylogeny may strongly constrain forest functioning (Carnicer et al.,
125 2013; Drobyshev et al., 2013) and induce different growth determinants among taxa (Genet et al.,
126 2010).

127 There is a gap between the knowledge obtained from global studies of universal C
128 allocation rules in forests and our understanding of the cell processes that underlie cambial
129 activity; currently, this gap appears to be the primary obstacle to a more complete understanding
130 of wood growth drivers. In this regard, species-specific studies that evaluate the dynamic of C
131 partitioning to annual wood growth along soil and climate gradients would be highly useful but
132 are lacking. Unfortunately, there is a scarcity of datasets that combine EC and growth
133 measurements at the same sites (Luyssaert et al., 2007). Here, we circumvented this limitation by
134 complementing stand and soil measurements at a French permanent plot network of 49 forest
135 sites with process-based simulations of annual and seasonal tree C balance (Fig. 1). Simulations
136 were performed using a process-based model (CASTANEA, Dufrêne *et al.* 2005) that was
137 thoroughly validated using EC data from throughout Europe (Davi et al., 2005; Delpierre et al.,
138 2009, 2012) and was applied using site-specific parameters. By relating biometric measurements
139 to variables that explain the C source and sink activity, we evaluated the key drivers of the annual
140 C allocation to stand wood growth in five species that are representative of the main European
141 forest biomes: *Fagus sylvatica*, *Quercus petraea* and *Quercus robur* for temperate deciduous
142 broadleaf forests; *Picea abies*, for high-latitude and high-altitude evergreen needleleaf forests;

143 and *Quercus ilex*, an evergreen broadleaf species from Mediterranean forests. Specifically, the
144 relative influence of annual and seasonal (from one month to the year) tree C balance (source
145 control), direct environmental control (water and temperature effects on sink activity) and
146 allocation adjustments related to age, past climate conditions, competition intensity and soil
147 nutrient availability on tree growth were considered (Fig. 1). We aimed to (1) quantify the
148 relative contributions of source and sink controls to the spatio-temporal dynamic of forest wood
149 growth across a wide range of environmental contexts and (2) provide information that can be
150 used to refine the representation of forest growth causalities in TBMs.

151

152 **2 Materials and methods**

153 We based our analyses on three complementary data sources: field measurements, climatic
154 variables from atmospheric reanalysis (Vidal et al., 2010) and process-based simulation data.
155 This hybrid approach allowed us to assess and disentangle the effects of previously reported
156 environmental and endogenous drivers of C allocation to wood growth (Fig. 1).

157

158 **2.1 Study sites and field data**

159 We gathered field measurements from 48 plots from the French Permanent Plot Network for the
160 Monitoring of Forest Ecosystems (RENECOFOR, Ulrich, 1997) and the Puéchabon tower flux
161 site (Martin-StPaul *et al.* 2013). The location and general climatic features of these plots are
162 shown in Fig. 2 and Table 1. Complete site description is available in Supplement S1.

163

164 **2.1.1 Growth measurements and historical stand growth reconstruction**

165 Growth measurements were obtained by two methods: *i*) Dendrochronological sampling, in
166 which 12 to 30 overstory trees per plot were cored to the pith at breast height with an incremental
167 borer. Cores were collected in 1994 at the RENECOFOR sites and in 2008 at the Puéchabon site
168 (Lebourgeois 1997; J.M. Ourcival, *unpublished data*). Tree circumferences at breast height

169 (CBHs) and total heights were also measured. The average stand age was inferred from the tree
170 ring series. *ii*) Forest inventories, in which extensive CBH surveys were conducted in a 0.5 ha
171 area of every plot (Cluzeau *et al.* 1998; Gaucherel, Guiot & Misson 2008; J.M. Ourcival,
172 unpublished data).

173 Tree ring series were combined with the CBH surveys to reconstruct the historical CBHs of every
174 tree on the plots (over 8 to 43 years, Supplement S1). The entire stand tree CBH distribution was
175 reconstructed from the CBHs of the sampled trees using an empirical tree competition model
176 (Deleuze *et al.*, 2004). This model stipulates that only trees with a CBH above a given threshold
177 (σ , the minimum circumference needed to gain direct access to sunlight), have a significant
178 growth. Overstory trees then have an annual basal area growth rate that is proportional to their
179 size, according to a slope coefficient, γ . Following the work of Guillemot *et al.* (2014), the model
180 was calibrated annually, beginning at year (n) of the core sampling and used iteratively to
181 reconstruct the past stand CBH growth. The σ parameter was first defined using an empirical
182 relationship with the maximum CBH of the stand tree distribution from year (n). The γ parameter
183 was then adjusted using the tree rings measured on the sampled trees in year (n-1). The
184 parameterized model was finally used to predict the basal area increments of all the trees in the
185 distribution, and consequently the tree CBH distribution in the year (n-1). A detailed description
186 of the iterative process can be found in Supplement S2 and in Guillemot *et al.* (2014).

187 The inferred past trajectory of the stand CBH distribution was used to calculate the historical
188 number of stems (*numstem*, Table 2) and stand basal area, which we considered to be a proxy for
189 within-stand competition intensity (*SBA*, Table 2, Kunstler *et al.* 2011). The historical total
190 woody stand biomass was also calculated (Supplement S3) using species-specific tree level
191 allometric functions (Bontemps *et al.*, 2009, 2012; Dhôte and Hercé, 1994; Seynave *et al.*, 2005;
192 Vallet *et al.*, 2006) and wood density models (Bouriaud *et al.*, 2004; Wilhelmsson *et al.*, 2002;
193 Zhang *et al.*, 1993). For *Q. ilex*, we used the appropriate function from Rambal *et al.* (2004) to
194 calculate the stand woody biomass from CBHs. Past annual woody biomass increments (AWBIs)
195 were then inferred (Supplement S4).

196

197 **2.1.2 Measurements of stand characteristics**

198 The stand measurements included the soil water holding capacity (SWHC), leaf area index (LAI),
199 leaf N content (LNC) and soil nutrient availability (SNA). The SWHC was estimated via the soil
200 depth and texture measured at two soil pits per plot (Brêthes and Ulrich, 1997). The LAI was
201 estimated from litter collection (Pasquet, 2002), and the sunlit LNC was determined annually for
202 8 trees between 1993 and 1997 (Croisé et al., 1999).

203 SNA was assessed as the soil's C:N biomass ratio, the absolute value of the cation-exchange
204 capacity and the per cent base saturation (Ponette, 1997). These soil indices were measured at 3
205 depths (0 to 10, 10 to 20, 20 to 40 cm) and were used to categorize the soil plots into three
206 nutrient classes, from low to high nutrient availability (Supplement S5). The SNA, SWHC and
207 LNC were used to characterize plot fertility in the statistical analyses (Table 2).

208

209 **2.2 Climate data**

210 The following meteorological variables at the hourly temporal scale (with 8km spatial resolution)
211 were obtained from the SAFRAN atmospheric reanalysis (Vidal et al., 2010): global radiation,
212 rainfall, wind speed, air humidity and air temperature. Temperature, which was related to the
213 average altitudes of the SAFRAN cells, was corrected using plot-specific elevation measurements
214 (assuming a lapse rate of 0.6 °K per 100 m, Supplement S1). These variables were used for
215 climate forcing in the CASTANEA model (Dufrêne *et al.* 2005, see the following section). In
216 addition, two annual temperature indices were used as proxies of winter frost damage and low
217 temperature stress during the growing period (*frost* and *templim_{gp}*, respectively, Table 2).

218

219 **2.3 Process-based simulation data**

220 We used the CASTANEA model to simulate an ensemble of diagnostic variables that are related
221 to the C source and sink activity of forest stands: the elementary components of the tree C
222 balance, bioclimatic water stress indices and the onset of the biomass growth. The eco-

223 physiological process-based CASTANEA model aims to simulate C and water fluxes and stocks
224 of a monospecific, same-aged forest stand on a rotation time scale. The hourly stand-atmosphere
225 C fluxes predicted by the CASTANEA model have been thoroughly validated using EC data
226 from throughout Europe (Davi et al., 2005; Delpierre et al., 2009, 2012). Importantly, the
227 biophysical hypotheses that were formalized in this model are able to reproduce the interplay of
228 the complex mechanisms that lead to inter-annual variability in the stand C balance (Delpierre et
229 al., 2012); modelling this interplay has been recognized as a substantial challenge for TBMs
230 (Keenan et al., 2012). A complete description of CASTANEA is provided in Dufrêne *et al.*
231 (2005), and subsequent modifications are described in Davi *et al.* (2009) and Delpierre *et al.*
232 (2012). For the purpose of the present study, CASTANEA was parameterized with site-specific
233 SWHC and LNC values. The measured LAI and total woody biomass were used to initialize the
234 model simulations. The model's ability to reproduce the annual variability in LAI and the forest
235 growth has been recently validated (Guillemot et al., 2014). Nevertheless, the annual standing
236 woody biomass was forced to conform to the observed values, because the model was used for
237 diagnostic purposes in this study.

238 Several groups of variables were simulated and aggregated on an annual basis (Table 2):

239 1. *The elementary components of the tree C balance.* These components included the GPP,
240 autotrophic respiration (R_a), and net balance (i.e., net primary productivity, $NPP = GPP -$
241 R_a). For a given year y , we aggregated the hourly simulated C fluxes over different
242 seasonal time periods, with starting days that ranged from 30 to 190 and ending days that
243 ranged from 190 to 350, at a 2-day resolution. The C fluxes were also summed i) for the
244 species-specific biomass growth periods reported in the literature (GPP_{gp} , $R_{a_{gp}}$ and
245 NPP_{gp} , Supplement S6) and ii) for the entire preceding year ($y-1$) as a proxy of the forest
246 C status induced by past climate conditions (lagged effect, GPP_{y-1} , $R_{a_{y-1}}$ and NPP_{y-1}).

247
248 2. *Bioclimatic water stress indices.* These indices included the intensity and duration of
249 water stress ($WS_{int_{gp}}$ and $WS_{per_{gp}}$, respectively, Supplement S7) during species-
250 specific growing periods that have been reported in the literature (Supplement S6). The
251 CASTANEA model simulated the daily soil water balance, based on a bucket soil sub-
252 model with 2 layers (a top soil layer and a total soil layer that includes the top soil layer,

253 Dufrêne et al., (2005)). $WS_{int_{gp}}$ was then used to quantify the intensity of water stress by
254 summing the *reduc* index on a daily basis (Granier et al., 1999).

255

$$256 \quad reduc_t = \max\left(0, \min\left(1, \frac{SWC_t - SWC_{wilt}}{0.4 \times (SWC_{fc} - SWC_{wilt})}\right)\right)$$

257

258 where SWC_t is the soil water content on day t (mm), SWC_{wilt} is the soil water content at
259 the wilting point (mm) and SWC_{fc} is the soil water content at field capacity (mm).

260 $WS_{per_{gp}}$ is the number of days of the current growth period during which the soil water
261 content was less than 60% of the soil water holding capacity (Table 2, modified from
262 Mund et al., (2010)). Water stress indices were also calculated for the entire preceding
263 year (lagged effect of water stress, $WS_{int_{y-1}}$ and $WS_{per_{y-1}}$).

264

265 3. *The onset of the biomass growth (camb_onset)*. We used a new growth-onset module
266 (David, (2011); N. Delpierre and N. K. Martin-StPaul, unpublished results) based on a
267 temperature sum trigger (Supplement S8).

268

269 **2.4 Statistical analyses**

270 **2.4.1 General overview**

271 Statistical analyses were conducted in three complementary steps for each studied species. (1)
272 We calculated the correlation of the AWBIs and the C fluxes (GPP, NPP and Ra) aggregated
273 seasonally (from 1 month to one year) to evaluate the relationship between the C supply and
274 annual biomass growth changes. (2) The dependences of the AWBIs on the C source and the sink
275 activity were evaluated on an inter-site spatial scale to determine the influence of the site
276 characteristics on biomass growth. The relationship between the age and C allocation to woody
277 biomass was also evaluated in this step. By using the age differences among sites, our
278 chronosequence included a large range of ages (including stands that ranged in age from
279 approximately 30 to 150 years-old, Table S1). (3) Finally, the drivers of AWBI were assessed

280 temporally to determine the factors that were responsible for variability in the inter-annual
281 biomass growth.

282 Because many environmental factors affect both forest sink and source activities, there may be
283 strong covariance among the tree C balance and proxies of environmental stress (Fatichi et al.,
284 2014) that could hamper the inferential power of classical statistical tests (Graham, 2003).
285 However, the explanatory variables used in this study generally had correlation coefficients of
286 less than 0.7, the level above which collinearity begins to severely affect model performance
287 (Dormann et al., 2013). One exception was the correlation of components of the tree C balance
288 (because $NPP = GPP - Ra$). Consequently, the tree C balance components were introduced one at
289 a time into the models. In addition, temporal growth dependencies were evaluated using the
290 random forest (RF) learning method (Breiman, 2001). A number of studies have empirically
291 demonstrated the effectiveness of RF at identifying the “true” predictors among a large number
292 of correlated candidate predictors (e.g., Archer and Kimes, 2008; Cutler et al., 2007; Genuer et
293 al., 2010). The explanatory variables considered in our spatial and temporal analyses are
294 presented in Table 2 and Fig. 1. Analyses were conducted with the R software (R Development
295 Core Team 2013), using the packages lme4 (Bates et al., 2007), randomForest (Liaw and Wiener,
296 2002) and MuMIn (Barton and Barton, 2014). Because *Quercus petraea* and *Quercus robur* are
297 difficult to distinguish in the field and have a high hybridization rate (Abadie et al., 2012), these
298 two species were grouped in the analyses and are hereafter collectively referred to as “temperate
299 oaks”.

300

301 **2.4.2 Correlations between growth and C fluxes**

302 Pearson correlations between the AWBIs and simulated C fluxes in different seasonal time
303 periods were calculated separately for each site. The highest median correlation value for each
304 species was retained and tested against zero using Wilcoxon signed rank tests. Critical
305 correlations (i.e., the threshold values for a significant difference with the retained maximum
306 correlation) were determined to evaluate the sensitivity of the correlation values to changes in the
307 C flux aggregation periods.

308

309 **2.4.3 Drivers of spatial variations in biomass growth**

310 The drivers of spatial variations in biomass growth were evaluated using multiple regression
311 models using an information-theoretic approach (Burnham and Anderson, 2002). The AWBIs
312 and the considered explanatory variables were averaged for each plot. The variables introduced
313 into the linear models were centred and scaled such that their normalized coefficient estimates
314 indicated the relative influence of the predictors on the AWBI. The elementary components of
315 tree C balance (NPP, GPP and Ra) were introduced one at a time into the models. For each
316 species, multiple regression models that contained all possible combinations of the explanatory
317 variables were fitted. The models were compared using the second-order Akaike information
318 criterion (AIC), and all models with an Akaike weight of at least 1% of the best approximating
319 (lowest AIC) model were considered to be plausible (Burnham and Anderson, 2002). Ultimately,
320 we retained the variables that appeared in at least 95% of the selected models. Models fitted using
321 *P. abies* data were restricted to a maximum of 3 explanatory variables because of the small
322 sample size (n=6, Table 1). *Q. ilex* (n=1) was not considered in the spatial analyses. The
323 uncertainty of the simulated C fluxes was assessed in the analyses using a bootstrap procedure
324 (Chernick, 2011): all linear models were fitted 1000 times, and at each iteration, the C flux values
325 were randomly sampled within the root mean square error of the CASTANEA simulations
326 (Supplement S9) to obtain a parameter estimate distribution for each variable. We finally retained
327 the explanatory variables with parameter estimate distributions that excluded the zero value at a
328 two-tailed probability level of 5%.

329

330 **2.4.4 Drivers of temporal variations in biomass growth**

331 A temporal analysis was conducted on the standardized AWBI series: a double-detrending
332 process was applied to each series based on an initial linear regression model, followed by fitting
333 a cubic smoothing spline with a 50% frequency response cut-off (Mérián et al., 2011). For
334 analysing the temporal variations in biomass growth we used an RF learning method (Breiman,
335 2001), which was possible because of the large sample size (n = 931 site-years). The RF learning

336 method is a non-parametric method that is used to rank the contribution of different explanatory
337 variables and evaluate their marginal effects on a variable of interest without assuming an *a*
338 *priori* dependence. The RF method combined 500 binary decision trees that were built using
339 bootstrap samples from the initial dataset. The decisions trees aimed to reduce the heterogeneity
340 of the explained variable in the resulting branches. For each of the 500 trees, the data that were
341 not involved in the tree construction were used for validation. The tree predictions and errors
342 were then averaged to provide the final RF results. The RF method does not overfit or require
343 cross-validation (Cutler et al., 2007). A subset of explanatory variables was randomly chosen at
344 each node, thus reducing the effect of collinear variables on the output. The RF method was used
345 to select variables that explained the temporal variability in biomass growth (Genuer et al., 2010).
346 Variable selection relied on permutation importance, i.e., the existence of an increase in the
347 global mean square error when a given variable was randomized in the validation subsamples.
348 The forms of the dependences were illustrated by partial dependence plots (graphical depiction of
349 the marginal effect of a given variable, Cutler *et al.* 2007). We used this information (variable
350 selection and dependence forms) to test for the significance of the temporal AWBI dependences
351 within the linear model. The uncertainty in the simulated C fluxes was considered in the linear
352 models, following the procedure described in the spatial analysis section.

353

354 **3 Results**

355 **3.1 Relationship between woody biomass growth and C fluxes**

356 The elementary components of the simulated seasonal tree C balance differed in terms of their
357 relationships with the inter-annual variability of the annual woody biomass increments (AWBI,
358 Table 3). The simulated seasonal GPP and NPP were linked to AWBIs with a comparable
359 agreement between species. However, the simulated Ra had weak and often non-significant
360 relationships with the AWBIs across the 49 studied plots. The strongest correlations were
361 obtained for flux aggregation periods that i) were generally consistent within a species for GPP
362 and NPP but different for Ra and ii) strongly differed among species (Table 3). The coefficients
363 of variation of the simulated annual NPP, GPP and Ra across the 49 studied sites were $10.8\% \pm 3$,
364 $7.4\% \pm 2$, and $6.8\% \pm 3$, respectively. GPP and NPP were summed from the beginning of May to

365 the beginning of August and September, in temperate oaks and *F. sylvatica*, respectively. The
366 longest GPP and NPP aggregation periods were obtained for *P. abies* (from the beginning of
367 February to mid-September), and the shortest period were found for *Q. ilex* (from the beginning
368 of July to mid-August). Minor (less than 20 days) changes in the flux aggregation period
369 associated with the maximum simulated flux-AWBI correlation usually marginally affected the
370 correlation values (Supplement S10). Consequently, aggregation periods that were less than 13
371 days different (either in terms of their starting or ending dates) from the values reported in Table
372 3 were generally not significantly lower than the maximum values (see the critical values
373 presented in Supplement S10).

374 **3.2 Spatial dynamic of C allocation to woody biomass growth**

375 The inter-site variability in biomass growth was well explained by the selected multiple
376 regression models ($R^2 \geq 0.6$). We highlighted that species varied in terms of their inter-site
377 dependences (Table 4). The simulated C supply during the growth period (GPP_{gp} , Table 2) was
378 positively correlated with biomass growth in *F. sylvatica* and *P. abies*, whereas there was no
379 significant relationship between the average AWBI and photosynthesis among sites for temperate
380 oaks (Fig. 3A). Notably, the final models did not include NPP_{gp} or Ra_{gp} for any species. The stand
381 age was an important driver of biomass growth in temperate oaks and *F. sylvatica*. The stand age
382 explained a substantial portion of the AWBI:C supply ratio in all species, although the
383 relationship was not significant for *P. abies* (Fig. 3B). The fraction of C sequestered in woody
384 biomass decreased with stand age (Table 4, Fig. 3B) and was reduced by half in temperate oaks
385 and *F. sylvatica* stands that were between 50 and 150 years of age (from 0.3 to 0.13 and from
386 0.25 to 0.1, respectively). Additionally, we identified a significant and positive effect of stand
387 basal area on both AWBI (Table 4) and the AWBI: GPP_{gp} ratio (*data not shown*) in temperate
388 oaks.

389

390 **3.3 Temporal dynamic of carbon allocation to woody biomass growth**

391 The ranking of the drivers of biomass growth obtained using the RF algorithm indicated that the
392 temporal AWBI dependences varied among species (Fig. 4). The growth of temperate deciduous

393 species was under a more complex environmental control than the growth of *P. abies* and *Q. ilex*,
394 with several variables explaining a substantial portion of the annual variability in AWBI (Fig.
395 4A, B). Simulated C supply (GPP_{gp}) was strongly related to the AWBI of temperate oaks and *F.*
396 *sylvatica* and, to a lesser extent, *P. abies* (Fig. 4A, B, C), with positive marginal effects (Fig. 5 a,
397 e, h). The duration of water stress during the growth period ($WS_{per_{gp}}$) was the predominant
398 driver of the AWBI variability of *Q. ilex*, and was also strongly related to growth in temperate
399 deciduous species. Low temperatures during the growth period ($templim_{gp}$) most substantially
400 affected *P. abies* and also explained a portion of the variability in AWBI of temperate oaks. The
401 simulated water and temperature stress indices had negative and quasi-linear marginal effects on
402 the AWBI (Fig 5). Finally, environmental lagged effects contributed substantially to the AWBI
403 variability in all species: the water stress intensity of the previous year ($WS_{int_{y-1}}$) affected the
404 growth of *F. sylvatica* and *Q. ilex*, whereas the simulated C supply of the previous year (GPP_{y-1})
405 affected temperate oaks and *P. abies*. Lagged effects generally revealed threshold in marginal
406 dependences, with a significant negative effect on AWBI only under high water stress or low C
407 supply (Fig. 5). The effects of the retained variables (Fig. 4) were evaluated via multiple
408 regression models that used dummy variables to test for the significance of slope changes when
409 thresholds appeared on partial plots (Fig. 5). The models explained approximately 20% of the
410 variability in the AWBI for temperate oaks and *P. abies*, and approximately 40% of the
411 variability for *F. sylvatica* and *Q. ilex* (Table 5). All of the explanatory variables had significant
412 effects, but $templim$ was not retained in the models for temperate oaks after the bootstrap
413 procedure that accounted for the uncertainty of the C flux simulations. We observed significant
414 changes in the slopes of the effect of GPP_{y-1} on temperate oaks and the effect of GPP_{gp} on *P.*
415 *abies* (Table 5). The models with NPP_{gp} and NPP_{y-1} variables revealed the same AWBI
416 dependences as the models described above, but with reduced explanatory power. The models
417 with Ra_{gp} and Ra_{y-1} variables were not significant (*data not shown*).

418

419 **4 Discussion**

420 This study quantified the C that is allocated annually to the woody biomass increment for five
421 species that are representative of the main European forest biomes. By complementing field
422 measurements from a permanent plot network with process-based modelling, our approach

423 circumvented the limitation of EC data scarcity and characterized the annual partitioning of C
424 into woody biomass at 49 sites over France (931 site-years). We were thus able to identify the
425 species-specific drivers of the spatiotemporal dynamics of the allocation of C to wood growth
426 along ecological gradients.

427

428 **4.1 The correlation between the tree C balance and woody biomass growth**

429 Relating EC-based estimates of forest C balance and biometric measurements of woody biomass
430 growth has been the focus of an increasing number of studies. These studies can enhance our
431 understanding of ecosystem C dynamics but have so far provided conflicting conclusions. Indeed,
432 the correlation between woody biomass growth and forest C gain has been reported as both non-
433 significant (Mund et al., 2010; Richardson et al., 2013; Rocha et al., 2006) and highly significant
434 (Babst et al., 2014; Ohtsuka et al., 2009; Peichl et al., 2010; Zweifel et al., 2010). Accordingly,
435 the relationships between AWBI and C fluxes reported in this study strongly varied among sites
436 for each of the species studied (Table 3). Nevertheless, the annual woody biomass increment was
437 consistently related to GPP_{gp} and NPP_{gp} , and only marginally to Ra_{gp} for the majority of sites
438 (Table 3). Babst et al. (2014) reported a similar dependence of biomass growth on C fluxes at 5
439 sites that spanned a wide range of latitude in Europe. The authors attributed this result to a
440 common sensitivity of C assimilation and biomass growth to the water balance. Our results also
441 support the view that biomass growth and tree C balance are under the control of distinct but
442 partially correlated processes (Beer et al., 2007; Fatichi et al., 2014); these processes may or may
443 not induce consistent annual changes, depending on the environmental conditions faced by trees.
444 For *F. sylvatica* and temperate oaks, maximum correlation values corresponded to flux
445 aggregation periods that were consistent with the previously reported phenology of the woody
446 biomass increment (Table 3, Michelot *et al.* 2012, Supplement S10). Babst et al. (2014) and
447 Granier et al. (2008) similarly reported close relationships between the AWBI and forest C fluxes
448 that were summed until cessation of growth (August/September). The flux aggregation periods
449 were, however, not related to the timing of wood growth in *Q. ilex* or *P. abies* (Cuny et al., 2012;
450 Lempereur et al., 2015), which indicates that inter-annual variation in the AWBI is not always
451 solely (or even primarily, e.g., *Q. ilex* and *P. abies*) dependent on the C derived from
452 photosynthesis. Specifically, the agreement between the observed annual growth and a short

453 period of C flux aggregation in early summer that was reported for *Q. ilex* corresponds to the
454 effect of growth cessation on the annual biomass increment, which has been attributed to a
455 drought-induced limitation of cambial activity at the Puéchabon site (Lempereur et al., 2015).
456 The processes that underlie the relationship of the long flux aggregation period and the annual
457 biomass increment of *P. abies* may include the effect of late winter temperature on cambium
458 phenology (Rossi et al., 2011). Overall, our results suggest that using growth-flux correlation
459 coefficients when investigating either source limitation of growth or the seasonality of C
460 allocation to woody biomass can lead to misleading conclusions.

461

462 **4.2 Between-site variability in the C allocation to woody biomass growth is** 463 **related to ontogeny and competition intensity**

464 We highlighted an age-related decline in the C partitioning to woody biomass in all three species
465 (Fig. 3B). This result had previously been observed in *F. sylvatica* stands using measurements of
466 the main C compartments along a chronosequence (Genet et al., 2010). Several non-exclusive
467 processes can explain this age-related trend. Increases in tree height are associated with increases
468 in the hydraulic resistance of xylem, which may lead to declines in the turgor of living cells and
469 result in potentially negative consequences on cambial activity (Woodruff et al., 2004). This
470 constraint may result in a height-related sink-limitation of growth (Woodruff and Meinzer, 2011),
471 which is consistent with our results. Additionally, life-history traits, such as a greater emphasis on
472 reproduction in older stands, could also be involved. However, the interactions of growth and
473 reproductive mechanisms are still under debate (Hoch et al., 2013; Thomas, 2011) and have yet
474 to be properly represented in TBMs. Only the GPP component of the simulated tree C balance
475 was retained in the final models (Table 4), thereby indicating that an increase in maintenance
476 respiration with greater stand biomass most likely did not contribute to the age-related decline in
477 biomass growth (Drake et al., 2011; Tang et al., 2014). Although height-related hydraulic
478 constraints on C assimilation have been suggested to be an important driver (Ryan et al., 2006;
479 Tang et al., 2014), recent studies have suggested that changes in demography and stand structure
480 may primarily explain the age-related decline observed in stand wood growth (Binkley et al.,
481 2002; Xu et al., 2012). Our results suggest that changes in the C allocation should also be
482 considered, because no mortality occurred in our plots during the measurement period (*data not*

483 *shown*). We additionally identified a significantly higher C partitioning to woody biomass in
484 temperate oak stands with greater competition intensity (i.e., high stand basal area, Table 3). To
485 date, reports regarding the effect of competition on C allocation dynamics are conflicting (Litton
486 et al., 2007) and suggest no significant or consistent effect. Moreover, we found no significant
487 effect of soil nutrient availability on the C allocation dynamics along the studied ecological
488 gradient whereas a recent meta-analysis reported that this factor positively affects C partitioning
489 to forest biomass on the global scale (Vicca et al., 2012). The RENECOFOR network only
490 includes relatively fertile sites (Supplement S5), which could putatively explain the apparent
491 tension between our results and the conclusions of the meta-analysis. Therefore, more studies are
492 required to elucidate the contributions of the various drivers to the variation in C partitioning to
493 woody biomass on scales that range from local to global.

494

495 **4.3 Inter-annual variability in woody biomass growth is consistent with** 496 **combined source-sink limitations**

497 Water and temperature stress exerted significant direct control on the inter-annual variation of
498 woody biomass growth (i.e., independently from their effects on C assimilation) for every species
499 and biome (Table 5 and Fig. 4 and 5). Cambial growth has been reported to be inhibited at lower
500 water stress levels than photosynthesis (Muller et al., 2011; Tardieu et al., 2011). Indeed,
501 drought-induced decrease in cell turgor strongly affects cell divisions (Woodruff and Meinzer,
502 2011) and cell wall expansion (Cosgrove, 2005; Lockhart, 1965) before gas exchange modulation
503 comes into play. Similarly, there is evidence that cell growth processes, such as cell division, are
504 more sensitive than photosynthesis to low temperatures (Körner, 2008). Although these findings
505 documented the plausible mechanisms of sink control of biomass growth at the cellular scale,
506 there is still considerable debate regarding whether the sink or the C source actually limit the
507 growth of the world's forests (Palacio et al., 2014; Wiley and Helliker, 2012). The typically
508 observed large C reserve pools (Hoch et al., 2003; Würth et al., 2005) have been interpreted as a
509 consequence of an overabundant C supply and thus evidence of sink control of tree growth
510 (Körner, 2003). However, recent works have suggested that a source limitation of growth may be
511 compatible with large C reserve pools if part of this mobile C is sequestered rather than stored
512 (Millard and Grelet, 2010) or if C storage is an active tree response to environmental stress

513 (Dietze et al., 2014; Wiley and Helliker, 2012). Using an alternative methodology (i.e. a
514 methodology that is not based on C storage measurement) our results suggest that sink limitation
515 has a significant effect on the annual woody biomass growth of five species that are
516 representative of different European biomes, including deciduous temperate forests. Because sink
517 limitation implies that there are periods with significant C supply but no growth, our results also
518 corroborate recent empirical studies that reported a significant role of growth duration in the
519 annual variability of tree radial increment (Brzostek et al., 2014; Cuny et al., 2012; Lempereur et
520 al., 2015). Additionally, we observed that past environmental constraints significantly affected C
521 partitioning to wood growth for each species and biome (Table 5 and Fig. 4 and 5). The lagged
522 effect of the previous year's low C supply (GPP_{y-1}) possibly indicates a preferential C allocation
523 to storage at the expense of growth in trees that face C reserve pool depletion (Bansal and
524 Germino, 2008; Wiley et al., 2013). In support of this finding, Richardson *et al.* (2012) reported a
525 strong relationship between the AWBI and the EC-based estimate of the previous year's C supply
526 in a mature maple stand. The detrimental effect of a previous year's low C supply on temperate
527 oak wood growth (Fig. 4) may be related to growth phenology, because this species relies on C
528 reserves to achieve a large part of its annual biomass growth prior to leaf expansion in the spring
529 (Barbaroux et al., 2003). The lagged effect of high water stress intensity on *F. sylvatica* and *Q.*
530 *ilex* (Fig. 4) may be linked to previous drought-induced mortalities of buds or fine roots
531 (Leuschner et al., 2001; López et al., 2003). Indeed, pre-built buds are thought to strongly
532 regulate the following year's cambial activity (Delpierre et al., 2015; Palacio et al., 2012; Zweifel
533 et al., 2006) and a recent meta-analysis concluded that C is preferentially allocated to fine roots at
534 the expense of wood growth in stands that face constraining environments (Chen et al., 2013).
535 Finally, our results suggest that C supply (GPP_{gp}) is an important driver of the annual woody
536 biomass growth in temperate deciduous forests (Daudet et al., 2005). GPP was the component of
537 the simulated tree C balance that was most closely related to the annual variability in growth; this
538 result indicates GPP's important role in explaining the annual variability in the net ecosystem
539 productivity of European forests (Delpierre et al., 2012). Overall, our findings support the
540 premise that forest woody biomass growth is subject to complex control processes that include
541 both source and sink limitations, following Liebig's law: although numerous processes
542 potentially influence wood growth, stand growth at a given site and a given year is predominantly
543 limited by the most constraining factor. C (source) limitation of growth can thus only occur when

544 other factors are non-limiting (Fatichi et al., 2014), a situation that is expected to be rare in
545 strongly constrained environment such as Mediterranean or mountainous areas (Fig. 4).

546

547 **4.4 Toward an integrated modelling framework**

548 Most models that are currently used to project the outcome of global changes on forests represent
549 wood growth as a fraction of the total C uptake (i.e., source control of growth, De Kauwe *et al.*
550 2014). This C-centric perspective overlooks the possibility of sink control of growth and thus
551 ignores results such as those presented in this study and those of earlier local studies (reviewed
552 by Fatichi *et al.* 2014). Consequently, this perspective possibly hampers the ability of TBMs to
553 project future forest productivity (Fatichi *et al.* 2014). On the basis of our analysis of the
554 spatiotemporal dynamics of C allocation to wood growth on a regional scale, we suggest a
555 straightforward, combined source- and sink-driven forest growth modelling framework (Fig. 6).
556 In this framework, a potential site-specific allocation coefficient is first defined to represent the
557 effect of soil fertility on the C allocation to wood (Vicca et al., 2012). In a second step, this
558 coefficient is adjusted to the physiological state of the stand by accounting for the dependences of
559 the C allocation on ontogeny, competition intensity and lagged environmental stressors. Lagged
560 environmental stressors are represented by a negative effect on the previous year's water stress
561 index and low C uptake on the allocation coefficient. The resulting potential allocation
562 coefficient is finally modulated on a daily basis by i) the phenology of wood growth, which
563 defines the onset and cessation of the growth period (Delpierre et al., 2015) and ii) the sink
564 limitations of wood growth: the coefficient value of a given day is calculated using the potential
565 coefficient value and the water and temperature stresses experienced during that day. The water
566 and temperature stresses induce day-to-day fluctuations in the allocation coefficient value that
567 represent the sink limitations of wood growth, i.e. the direct effect of water and temperature
568 stresses on growth. The framework presented here is a calibration strategy that requires field data
569 to be implemented in TBMs. Our results can help defining the forms of the coefficient
570 dependences that will be formalized in the next generation of models (Figs. 3 and 5).

571 Our approach can be seen as an intermediate step toward a more mechanistic
572 representation of C allocation to woody biomass (Hölttä et al., 2010; Schiestl-Aalto et al., 2015).

573 It synthesizes the current knowledge regarding forest growth dependences and has the potential to
574 unify seemingly contradictory observations within a single modelling framework. The simulated
575 growth is indeed subject to the combined controls of C supply and changes in C allocation due to
576 endogenous adjustments and/or modulations of sink activity (Fig. 6). These controls result from
577 distinct processes, which are independently represented in the modelling framework. The relative
578 influences of the various processes, i.e., the simulated growth causalities, are thus likely to vary
579 both spatially and temporally, depending on the environmental conditions faced by trees. Our
580 approach has therefore the potential to shed light on the contrasted results reported by correlative
581 studies. Although the value is comparable to those of previous studies (Lebourgeois et al., 2005;
582 Mérian et al., 2011), the proportion of the annual growth variability that was explained by our
583 approach was moderate (Table 5). Plausible explanations of this result include: i) unreported
584 management interventions that may have skewed the historical stand growth reconstruction and
585 ii) potentially important growth drivers that were not considered here, such as changes in C
586 partitioning due to mast seeding (Mund et al., 2010), genetic differentiation among tree
587 populations (Vitasse et al., 2014) or allometry-mediated tree acclimation to drought (Martin-
588 StPaul et al., 2013). A third factor that hampered the ability of our empirical models to explain
589 the annual growth variability is the potential disagreement between the CASTANEA outputs that
590 were used as explanatory variables and the corresponding actual drivers. Although we argued that
591 i) the CASTANEA model has been thoroughly validated at many EC sites from throughout
592 Europe and ii) the presented growth dependences demonstrated their robustness against the
593 reported uncertainties of the CASTANEA simulations, the quality of the simulations was limited
594 by the idiosyncrasies of the sites we examined in this study. In particular, a number of past
595 disturbances such as insect outbreaks, windthrow or unreported commercial thinning could have
596 temporarily induced large discrepancies between the actual and simulated C fluxes (Grote et al.,
597 2011; Hicke et al., 2012). The error that is attributable to model performance unfortunately
598 remains unknown because of the absence of EC measurements at our study sites (except for the
599 Puéchabon site, see Delpierre et al., 2012). Despite this additional uncertainty, the combined use
600 of field measurements and process-based modelling allowed us to present the first species-
601 specific evaluation of annual C allocation to growth along regional environmental gradients. Our
602 results suggest that implementing the presented C allocation dependences in TBMs will refine the
603 projections of the outcome of global changes on forest growth, and have implications for the

604 predicted evolution of forest C sink, forest diebacks and tree species distributions (Cheaib et al.,
605 2012).

606

607

608 **Acknowledgements**

609 We wish to thank the Office National des Forêts and the RENECOFOR network team,
610 particularly Manuel Nicolas and Marc Lanier, for providing the RENECOFOR database. The
611 SAFRAN database was provided by Météo-France as part of the HYMEX project. J.G. received a
612 PhD grant from the French Ministère de l'Enseignement Supérieur et de la Recherche and the
613 University of Paris-Sud. A post-doctoral research grant to N.K.M.-S. was provided by the
614 Humboldt project within the GIS Climat. As part as the ICP forests network data (icp-forests.net),
615 the material used in this article is available, free of charge, upon request (please contact M.
616 Nicolas, manuel.nicolas@onf.fr, +00331 60 74 92 28, Office National des Forêts, Fontainebleau,
617 F-77300, France).

618

619 **References**

620 Abadie, P., Roussel, G., Dencausse, B., Bonnet, C., Bertocchi, E., Louvet, J., Kremer, A. and
621 Garnier-Géré, P.: Strength, diversity and plasticity of postmating reproductive barriers between
622 two hybridizing oak species (*Quercus robur* L. and *Quercus petraea* (Matt) Liebl.), *J. Evol. Biol.*,
623 25(1), 157–173, 2012.

624 Archer, K. J. and Kimes, R. V: Empirical characterization of random forest variable importance
625 measures, *Comput. Stat. Data Anal.*, 52(4), 2249–2260, 2008.

626 Babst, F., Bouriaud, O., Papale, D., Gielen, B., Janssens, I. A., Nikinmaa, E., Ibrom, A., Wu, J.,
627 Bernhofer, C., Köstner, B., Grünwald, T., Seufert, G., Ciais, P. and Frank, D.: Above-ground
628 woody carbon sequestration measured from tree rings is coherent with net ecosystem
629 productivity at five eddy-covariance sites, *New Phytol.*, 201(4), 1289–1303,
630 doi:10.1111/nph.12589, 2014.

631 Bansal, S. and Germino, M. J.: Carbon balance of conifer seedlings at timberline: relative
632 changes in uptake, storage, and utilization., *Oecologia*, 158(2), 217–27, doi:10.1007/s00442-
633 008-1145-4, 2008.

634 Barbaroux, C., Breda, N. and Dufrene, E.: Distribution of above-ground and below-ground
635 carbohydrate reserves in adult trees of two contrasting broad-leaved species (*Quercus petraea*
636 and *Fagus sylvatica*), *New Phytol.*, 157(3), 605–615 [online] Available from:
637 <http://doi.wiley.com/10.1046/j.1469-8137.2003.00681.x>, 2003.

638 Barton, K. and Barton, M. K.: Package “MuMIn,” Version, 1, 18, 2014.

639 Bates, D., Sarkar, D., Bates, M. D. and Matrix, L.: The lme4 package, *R Packag. version*, 2(1),
640 2007.

- 641 Beer, C., Reichstein, M., Ciais, P., Farquhar, G. D. and Papale, D.: Mean annual GPP of Europe
642 derived from its water balance, *Geophys. Res. Lett.*, 34(5), 2007.
- 643 Binkley, D., Stape, J. L., Ryan, M. G., Barnard, H. R. and Fownes, J.: Age-related Decline in
644 Forest Ecosystem Growth: An Individual-Tree, Stand-Structure Hypothesis, *Ecosystems*, 5(1),
645 58–67, doi:10.1007/s10021-001-0055-7, 2002.
- 646 Bontemps, J.-D., Hervé, J.-C. and Dhôte, J.-F.: Long-term changes in forest productivity: a
647 consistent assessment in even-aged stands, *For. Sci.*, 55(6), 549–564, 2009.
- 648 Bontemps, J.-D., Herve, J.-C., Duplat, P. and Dhôte, J.-F.: Shifts in the height-related
649 competitiveness of tree species following recent climate warming and implications for tree
650 community composition: the case of common beech and sessile oak as predominant
651 broadleaved species in Europe, *Oikos*, 121(8), 1287–1299, doi:10.1111/j.1600-
652 0706.2011.20080.x, 2012.
- 653 Bouriaud, O., Bréda, N., Le Moguédec, G. and Nepveu, G.: Modelling variability of wood density
654 in beech as affected by ring age, radial growth and climate, *Trees - Struct. Funct.*, 18(3), 264–
655 276, doi:10.1007/s00468-003-0303-x, 2004.
- 656 Breiman, L.: Random forests, *Mach. Learn.*, 45(1), 5–32, 2001.
- 657 Brêthes, A. and Ulrich, E.: RENECOFOR - Caractéristiques pédologiques des 102 peuplements
658 du réseau., Off. Natl. des forêts, Département des Rech. Tech., 1997.
- 659 Brüggemann, N., Gessler, a., Kayler, Z., Keel, S. G., Badeck, F., Barthel, M., Boeckx, P.,
660 Buchmann, N., Brugnoli, E., Esperschütz, J., Gavrishkova, O., Ghashghaie, J., Gomez-
661 Casanovas, N., Keitel, C., Knohl, a., Kuptz, D., Palacio, S., Salmon, Y., Uchida, Y. and Bahn,
662 M.: Carbon allocation and carbon isotope fluxes in the plant-soil-atmosphere continuum: a
663 review, *Biogeosciences*, 8(11), 3457–3489, doi:10.5194/bg-8-3457-2011, 2011.
- 664 Brzostek, E. R., Dragoni, D., Schmid, H. P., Rahman, a F., Sims, D., Wayson, C. a, Johnson, D.
665 J. and Phillips, R. P.: Chronic water stress reduces tree growth and the carbon sink of deciduous
666 hardwood forests., *Glob. Chang. Biol.*, doi: 10.1111/gcb.12528, doi:10.1111/gcb.12528, 2014.
- 667 Burnham, K. P. and Anderson, D. R.: Model selection and multi-model inference: a practical
668 information-theoretic approach, Springer., 2002.
- 669 Carnicer, J., Barbeta, A., Sperlich, D., Coll, M. and Peñuelas, J.: Contrasting trait syndromes in
670 angiosperms and conifers are associated with different responses of tree growth to temperature
671 on a large scale., *Front. Plant Sci.*, 4(October), 409, doi:10.3389/fpls.2013.00409, 2013.
- 672 Carvalhais, N., Forkel, M., Khomik, M., Bellarby, J., Jung, M., Migliavacca, M., Mu, M., Saatchi,
673 S., Santoro, M. and Thurner, M.: Global covariation of carbon turnover times with climate in
674 terrestrial ecosystems, *Nature*, 2014.
- 675 Chapin, F. S., Schulze, E.-D. and Mooney, H. A.: The ecology and economics of storage in
676 plants, *Annu. Rev. Ecol. Syst.*, 21, 423–447, 1990.

677 Cheaib, A., Badeau, V., Boe, J., Chuine, I., Delire, C., Dufrêne, E., François, C., Gritti, E. S.,
678 Legay, M., Pagé, C., Thuiller, W., Viovy, N. and Leadley, P.: Climate change impacts on tree
679 ranges: model intercomparison facilitates understanding and quantification of uncertainty., *Ecol.*
680 *Lett.*, 15(6), 533–44, doi:10.1111/j.1461-0248.2012.01764.x, 2012.

681 Chen, G., Yang, Y. and Robinson, D.: Allocation of gross primary production in forest
682 ecosystems: allometric constraints and environmental responses, *New Phytol.*, 200(4), 1176–
683 1186, 2013.

684 Chernick, M. R.: *Bootstrap methods: A guide for practitioners and researchers*, Wiley., 2011.

685 Clark, D. B., Mercado, L. M., Sitch, S., Jones, C. D., Gedney, N., Best, M. J., Pryor, M., Rooney,
686 G. G., Essery, R. L. H., Blyth, E., Boucher, O., Harding, R. J., Huntingford, C. and Cox, P. M.:
687 The Joint UK Land Environment Simulator (JULES), model description – Part 2: Carbon fluxes
688 and vegetation dynamics, *Geosci. Model Dev.*, 4(3), 701–722, doi:10.5194/gmd-4-701-2011,
689 2011.

690 Cluzeau, C., Ulrich, E., Lanier, M. and Garnier, F.: *RENECOFOR - Interprétation des mesures*
691 *dendrométriques de 1991 à 1995 des 102 peuplements du réseau*, Off. Natl. des forêts,
692 Département des Rech. Tech., 1998.

693 Cosgrove, D. J.: Growth of the plant cell wall., *Nat. Rev. Mol. Cell Biol.*, 6(11), 850–61,
694 doi:10.1038/nrm1746, 2005.

695 Croisé, L., Cluzeau, C., Ulrich, E., Lanier, M. and Gomez, A.: *RENECOFOR - Interprétation des*
696 *analyses foliaires réalisées dans les 102 peuplements du réseau de 1993 a 1997 et premières*
697 *évaluations interdisciplinaires*, Off. Natl. des forêts, Département des Rech. Tech., 1999.

698 Cuny, H. E., Rathgeber, C. B. K., Lebourgeois, F., Fortin, M. and Fournier, M.: Life strategies in
699 intra-annual dynamics of wood formation: example of three conifer species in a temperate forest
700 in north-east France, *Tree Physiol.*, 32(5), 612–625, 2012.

701 Cutler, D. R., Edwards, T. C., Beard, K. H., Cutler, a and Hess, K. T.: Random forests for
702 classification in ecology, *Ecology*, 88(11), 2783–2792, 2007.

703 Daudet, F.-A., Améglio, T., Cochard, H., Archilla, O. and Lacoïnte, A.: Experimental analysis of
704 the role of water and carbon in tree stem diameter variations, *J. Exp. Bot.*, 56(409), 135–144,
705 2005.

706 Davi, H., Barbaroux, C., Francois, C. and Dufrene, E.: The fundamental role of reserves and
707 hydraulic constraints in predicting LAI and carbon allocation in forests, *Agric. For. Meteorol.*,
708 149(2), 349–361, doi:10.1016/j.agrformet.2008.08.014, 2009.

709 Davi, H., Dufrêne, E., Granier, a., Le Dantec, V., Barbaroux, C., François, C. and Bréda, N.:
710 Modelling carbon and water cycles in a beech forest, *Ecol. Modell.*, 185(2-4), 387–405,
711 doi:10.1016/j.ecolmodel.2005.01.003, 2005.

712 David, A.: *Modélisation de la croissance ligneuse chez le Hêtre et le Chêne sessile*. Master's
713 thesis dissertation, Université Paris-Sud, Orsay., 2011.

- 714 Deleuze, C., Pain, O., Dhôte, J. F. and Hervé, J. C.: A flexible radial increment model for
715 individual trees in pure even-aged stands, *Ann. For. Sci.*, 61(4), 327–335, doi:10.1051/forest,
716 2004.
- 717 Delpierre, N., Soudani, K., François, C., Köstner, B., Pontailier, J.-Y., Nikinmaa, E., Misson, L.,
718 Aubinet, M., Bernhofer, C., Granier, a., Grünwald, T., Heinesch, B., Longdoz, B., Ourcival, J.-M.,
719 Rambal, S., Vesala, T. and Dufrêne, E.: Exceptional carbon uptake in European forests during
720 the warm spring of 2007: a data-model analysis, *Glob. Chang. Biol.*, 15(6), 1455–1474,
721 doi:10.1111/j.1365-2486.2008.01835.x, 2009.
- 722 Delpierre, N., Soudani, K., François, C., Le Maire, G., Bernhofer, C., Kutsch, W., Misson, L.,
723 Rambal, S., Vesala, T. and Dufrêne, E.: Quantifying the influence of climate and biological
724 drivers on the interannual variability of carbon exchanges in European forests through process-
725 based modelling, *Agric. For. Meteorol.*, 154-155, 99–112, doi:10.1016/j.agrformet.2011.10.010,
726 2012.
- 727 Delpierre, N., Vitasse, Y., Chuine, I., Guillemot, J., Bazot, S., Rutishauser, T. and Rathgeber, C.
728 B. K.: Temperate and boreal forest tree phenology: from organ-scale processes to terrestrial
729 ecosystem models, *Ann. For. Sci.*, doi:10.1007/s13595-015-0477-6, 2015.
- 730 Dhôte, J.-F. and Hercé, É. de: Un modèle hyperbolique pour l'ajustement de faisceaux de
731 courbes hauteur-diamètre, *Can. J. For. Res.*, 24(9), 1782–1790, 1994.
- 732 Dietze, M. C., Sala, A., Carbone, M. S., Czimczik, C. I., Mantooth, J. A., Richardson, A. D. and
733 Vargas, R.: Nonstructural Carbon in Woody Plants, *Annu. Rev. Plant Biol.*, 65(1), 667–687,
734 doi:10.1146/annurev-arplant-050213-040054, 2014.
- 735 Dormann, C. F., Elith, J., Bacher, S., Buchmann, C., Carl, G., Carré, G., Marquéz, J. R. G.,
736 Gruber, B., Lafourcade, B. and Leitão, P. J.: Collinearity: a review of methods to deal with it and
737 a simulation study evaluating their performance, *Ecography (Cop.)*, 36(1), 27–46, 2013.
- 738 Drake, J. E., Davis, S. C., Raetz, L. M. and DeLucia, E. H.: Mechanisms of age-related changes
739 in forest production: the influence of physiological and successional changes, *Glob. Chang.*
740 *Biol.*, 17(4), 1522–1535, doi:10.1111/j.1365-2486.2010.02342.x, 2011.
- 741 Drobyshev, I., Gewehr, S., Berninger, F. and Bergeron, Y.: Species specific growth responses of
742 black spruce and trembling aspen may enhance resilience of boreal forest to climate change, *J.*
743 *Ecol.*, 101(1), 231–242, 2013.
- 744 Dufrêne, E., Davi, H., Francois, C., Le Maire, G., Le Dantec, V. and Granier, A.: Modelling
745 carbon and water cycles in a Beech forest. Part I: Model description and uncertainty analysis on
746 modelled NEE, *Ecol. Modell.*, 185(2-4), 407–436, doi:10.1016/j.ecolmodel.2005.01.004, 2005.
- 747 Fatichi, S., Leuzinger, S. and Körner, C.: Moving beyond photosynthesis: from carbon source to
748 sink-driven vegetation modeling, *New Phytol.*, 201(4), 1086–1095, doi:10.1111/nph.12614,
749 2014.
- 750 Franklin, O., Johansson, J., Dewar, R. C., Dieckmann, U., McMurtrie, R. E., Brännström, Å. and
751 Dybzinski, R.: Modeling carbon allocation in trees: a search for principles, *Tree Physiol.*, 32(6),
752 648–666, 2012.

- 753 Friend, A. D., Lucht, W., Rademacher, T. T., Keribin, R., Betts, R., Cadule, P., Ciais, P., Clark,
754 D. B., Dankers, R., Falloon, P. D., Ito, A., Kahana, R., Kleidon, A., Lomas, M. R., Nishina, K.,
755 Ostberg, S., Pavlick, R., Peylin, P., Schaphoff, S., Vuichard, N., Warszawski, L., Wiltshire, A.
756 and Woodward, F. I.: Carbon residence time dominates uncertainty in terrestrial vegetation
757 responses to future climate and atmospheric CO₂, *Proc. Natl. Acad. Sci.*, doi:
758 10.1073/pnas.1222477110, doi:10.1073/pnas.1222477110, 2013.
- 759 Gaucherel, C., Guiot, J. and Misson, L.: Changes of the potential distribution area of French
760 Mediterranean forests under global warming, *Biogeosciences*, 5(6), 1493–1504, 2008.
- 761 Genet, H., Bréda, N. and Dufrêne, E.: Age-related variation in carbon allocation at tree and
762 stand scales in beech (*Fagus sylvatica* L.) and sessile oak (*Quercus petraea* (Matt.) Liebl.) using
763 a chronosequence approach., *Tree Physiol.*, 30(2), 177–92, doi:10.1093/treephys/tpp105, 2010.
- 764 Genuer, R., Poggi, J.-M. and Tuleau-Malot, C.: Variable selection using random forests, *Pattern
765 Recognit. Lett.*, 31(14), 2225–2236, 2010.
- 766 Gielen, B., De Vos, B., Campioli, M., Neiryneck, J., Papale, D., Verstraeten, a., Ceulemans, R.
767 and Janssens, I. a.: Biometric and eddy covariance-based assessment of decadal carbon
768 sequestration of a temperate Scots pine forest, *Agric. For. Meteorol.*, 174-175, 135–143,
769 doi:10.1016/j.agrformet.2013.02.008, 2013.
- 770 Gough, C. M., Flower, C. E., Vogel, C. S., Dragoni, D. and Curtis, P. S.: Whole-ecosystem labile
771 carbon production in a north temperate deciduous forest, *Agric. For. Meteorol.*, 149(9), 1531–
772 1540, doi:10.1016/j.agrformet.2009.04.006, 2009.
- 773 Graham, M. H.: Confronting multicollinearity in ecological multiple regression, *Ecology*, 84(11),
774 2809–2815, 2003.
- 775 Granier, A., Bréda, N., Biron, P. and Villette, S.: A lumped water balance model to evaluate
776 duration and intensity of drought constraints in forest stands, *Ecol. Modell.*, 116(2), 269–283,
777 1999.
- 778 Granier, A., Bréda, N., Longdoz, B., Gross, P. and Ngao, J.: Ten years of fluxes and stand
779 growth in a young beech forest at Hesse, North-eastern France, *Ann. For. Sci.*, 64(7), 704–704
780 [online] Available from: <http://www.springerlink.com/index/HX4J1005V68TK726.pdf>, 2008.
- 781 Grote, R., Kiese, R., Grünwald, T., Ourcival, J.-M. and Granier, A.: Modelling forest carbon
782 balances considering tree mortality and removal, *Agric. For. Meteorol.*, 151(2), 179–190,
783 doi:10.1016/j.agrformet.2010.10.002, 2011.
- 784 Guillemot, J., Delpierre, N., Vallet, P., François, C., Martin-StPaul, N. K., Soudani, K., Nicolas,
785 M., Badeau, V. and Dufrêne, E.: Assessing the effects of management on forest growth across
786 France: insights from a new functional–structural model, *Ann. Bot.*, 114(4), 779–793,
787 doi:10.1093/aob/mcu059, 2014.
- 788 Hicke, J. A., Allen, C. D., Desai, A. R., Dietze, M. C., Hall, R. J., Kashian, D. M., Moore, D.,
789 Raffa, K. F., Sturrock, R. N. and Vogelmann, J.: Effects of biotic disturbances on forest carbon
790 cycling in the United States and Canada, *Glob. Chang. Biol.*, 18(1), 7–34, 2012.

- 791 Hoch, G., Richter, A. and Körner, C.: Non-structural carbon compounds in temperate forest
792 trees, *Plant. Cell Environ.*, 26(7), 1067–1081, 2003.
- 793 Hoch, G., Siegwolf, R. T. W., Keel, S. G., Körner, C. and Han, Q.: Fruit production in three
794 mastig tree species does not rely on stored carbon reserves., *Oecologia*, 171(3), 653–62,
795 doi:10.1007/s00442-012-2579-2, 2013.
- 796 Hölttä, T., Mäkinen, H., Nöjd, P., Mäkelä, A. and Nikinmaa, E.: A physiological model of
797 softwood cambial growth., *Tree Physiol.*, 30(10), 1235–52, doi:10.1093/treephys/tpq068, 2010.
- 798 De Kauwe, M. G., Medlyn, B. E., Zaehle, S., Walker, A. P., Dietze, M. C., Wang, Y., Luo, Y.,
799 Jain, A. K., El-Masri, B. and Hickler, T.: Where does the carbon go? A model–data
800 intercomparison of vegetation carbon allocation and turnover processes at two temperate forest
801 free-air CO₂ enrichment sites, *New Phytol.*, doi: 10.1111/nph.12847, 2014.
- 802 Keenan, T. F., Baker, I., Barr, A., Ciais, P., Davis, K., Dietze, M., Dragoni, D., Gough, C. M.,
803 Grant, R. and Hollinger, D.: Terrestrial biosphere model performance for inter-annual variability
804 of land-atmosphere CO₂ exchange, *Glob. Chang. Biol.*, 18(6), 1971–1987, 2012.
- 805 Keyes, M. R. and Grier, C. C.: Above- and below-ground net production in 40-year-old Douglas-
806 fir stands on low and high productivity sites, *Can. J. For. Res.*, 11(3), 599–605, doi:10.1139/x81-
807 082, 1981.
- 808 Körner, C.: Carbon limitation in trees, *J. Ecol.*, 91(1), 4–17 [online] Available from:
809 <http://www.blackwell-synergy.com/links/doi/10.1046%2Fj.1365-2745.2003.00742.x>, 2003.
- 810 Körner, C.: Winter crop growth at low temperature may hold the answer for alpine treeline
811 formation, *Plant Ecol. Divers.*, 1(1), 3–11, doi:10.1080/17550870802273411, 2008.
- 812 Krinner, G., Viovy, N., de Noblet-Ducoudré, N., Ogée, J., Polcher, J., Friedlingstein, P., Ciais, P.,
813 Sitch, S. and Prentice, I. C.: A dynamic global vegetation model for studies of the coupled
814 atmosphere-biosphere system, *Global Biogeochem. Cycles*, 19(1), 2005.
- 815 Kudo, K., Nabeshima, E., Begum, S., Yamagishi, Y., Nakaba, S., Oribe, Y., Yasue, K. and
816 Funada, R.: The effects of localized heating and disbudding on cambial reactivation and
817 formation of earlywood vessels in seedlings of the deciduous ring-porous hardwood, *Quercus*
818 *serrata*, *Ann. Bot.*, 113 (6), 1021–1027 [online] Available from:
819 <http://aob.oxfordjournals.org/content/113/6/1021.abstract>, 2014.
- 820 Kunstler, G., Albert, C. H., Courbaud, B., Lavergne, S., Thuiller, W., Vieilledent, G.,
821 Zimmermann, N. E. and Coomes, D. a.: Effects of competition on tree radial-growth vary in
822 importance but not in intensity along climatic gradients, *J. Ecol.*, 99(1), 300–312,
823 doi:10.1111/j.1365-2745.2010.01751.x, 2011.
- 824 Lebourgeois, F.: RENECOFOR - Etude dendrochronologique des 102 peuplements du réseau,
825 Off. Natl. des forêts, Département des Rech. Tech., 1997.
- 826 Lebourgeois, F., Bréda, N., Ulrich, E. and Granier, A.: Climate-tree-growth relationships of
827 European beech (*Fagus sylvatica* L.) in the French Permanent Plot Network (RENECOFOR),
828 *Trees*, 19(4), 385–401, doi:10.1007/s00468-004-0397-9, 2005.

- 829 Lempereur, M., Martin-StPaul, N. K., Damesin, C., Joffre, R., Ourcival, J. M., Rocheteau, A. and
830 Rambal, S.: Growth duration is a better predictor of stem increment than carbon supply in a
831 Mediterranean oak forest: implications for assessing forest productivity under climate change,
832 *New Phytol.*, In press, doi:10.1111/nph.13400, 2015.
- 833 Leuschner, C., Backes, K., Hertel, D., Schipka, F., Schmitt, U., Terborg, O. and Runge, M.:
834 Drought responses at leaf, stem and fine root levels of competitive *Fagus sylvatica* L. and
835 *Quercus petraea* (Matt.) Liebl. trees in dry and wet years, *For. Ecol. Manage.*, 149(1), 33–46,
836 2001.
- 837 Leuzinger, S. and Hättenschwiler, S.: Beyond global change: lessons from 25 years of CO₂
838 research., *Oecologia*, 171(3), 639–51, doi:10.1007/s00442-012-2584-5, 2013.
- 839 Leuzinger, S., Manusch, C., Bugmann, H. and Wolf, A.: A sink-limited growth model improves
840 biomass estimation along boreal and alpine tree lines, *Glob. Ecol. Biogeogr.*, 22(8), 924–932,
841 doi:10.1111/geb.12047, 2013.
- 842 Liaw, A. and Wiener, M.: The randomforest package, *R News*, 2(3), 18–22, 2002.
- 843 Litton, C. M., Raich, J. W. and Ryan, M. G.: Carbon allocation in forest ecosystems, *Glob.*
844 *Chang. Biol.*, 13(10), 2089–2109, doi:10.1111/j.1365-2486.2007.01420.x, 2007.
- 845 Lockhart, J. A.: An analysis of irreversible plant cell elongation, *J. Theor. Biol.*, 8(2), 264–275,
846 1965.
- 847 López, B. C., Sabate, S. and Gracia, C. A.: Thinning effects on carbon allocation to fine roots in
848 a *Quercus ilex* forest, *Tree Physiol.*, 23 (17), 1217–1224, doi:10.1093/treephys/23.17.1217,
849 2003.
- 850 Lupi, C., Morin, H., Deslauriers, A. and Rossi, S.: Xylem phenology and wood production:
851 resolving the chicken-or-egg dilemma., *Plant. Cell Environ.*, 33(10), 1721–30,
852 doi:10.1111/j.1365-3040.2010.02176.x, 2010.
- 853 Luysaert, S., Inglima, I., Jung, M., Richardson, a. D., Reichstein, M., Papale, D., Piao, S. L.,
854 Schulze, E.-D., Wingate, L., Matteucci, G., Aragao, L., Aubinet, M., Beer, C., Bernhofer, C.,
855 Black, K. G., Bonal, D., Bonnefond, J.-M., Chambers, J., Ciais, P., Cook, B., Davis, K. J.,
856 Dolman, a. J., Gielen, B., Goulden, M., Grace, J., Granier, A., Grelle, A., Griffis, T., Grünwald, T.,
857 Guidolotti, G., Hanson, P. J., Harding, R., Hollinger, D. Y., Hutyra, L. R., Kolari, P., Kruijt, B.,
858 Kutsch, W., Lagergren, F., Laurila, T., Law, B. E., Le Maire, G., Lindroth, A., Loustau, D., Malhi,
859 Y., Mateus, J., Migliavacca, M., Misson, L., Montagnani, L., Moncrieff, J., Moors, E., Munger, J.
860 W., Nikinmaa, E., Ollinger, S. V., Pita, G., Rebmann, C., Roupsard, O., Saigusa, N., Sanz, M. J.,
861 Seufert, G., Sierra, C., Smith, M.-L., Tang, J., Valentini, R., Vesala, T. and Janssens, I. A.: CO₂
862 balance of boreal, temperate, and tropical forests derived from a global database, *Glob. Chang.*
863 *Biol.*, 13(12), 2509–2537, doi:10.1111/j.1365-2486.2007.01439.x, 2007.
- 864 Magnani, F., Mencuccini, M. and Grace, J.: Age-related decline in stand productivity: the role of
865 structural acclimation under hydraulic constraints, *Plant. Cell Environ.*, 23(3), 251–263, 2000.
- 866 Martin-StPaul, N. K., Limousin, J.-M., Vogt-Schilb, H., Rodríguez-Calcerrada, J., Rambal, S.,
867 Longepierre, D. and Misson, L.: The temporal response to drought in a Mediterranean evergreen

- 868 tree: comparing a regional precipitation gradient and a throughfall exclusion experiment., *Glob.*
869 *Chang. Biol.*, 19(8), 2413–26, doi:10.1111/gcb.12215, 2013.
- 870 Mérian, P., Bontemps, J.-D., Bergès, L. and Lebourgeois, F.: Spatial variation and temporal
871 instability in climate-growth relationships of sessile oak (*Quercus petraea* [Matt.] Liebl.) under
872 temperate conditions, *Plant Ecol.*, 212(11), 1855–1871, doi:10.1007/s11258-011-9959-2, 2011.
- 873 Michelot, A., Simard, S., Rathgeber, C., Dufrêne, E. and Damesin, C.: Comparing the intra-
874 annual wood formation of three European species (*Fagus sylvatica*, *Quercus petraea* and *Pinus*
875 *sylvestris*) as related to leaf phenology and non-structural carbohydrate dynamics., *Tree*
876 *Physiol.*, 32(8), 1033–45, doi:10.1093/treephys/tps052, 2012.
- 877 Millard, P. and Grelet, G.-A.: Nitrogen storage and remobilization by trees: ecophysiological
878 relevance in a changing world., *Tree Physiol.*, 30(9), 1083–95, doi:10.1093/treephys/tpq042,
879 2010.
- 880 Muller, B., Pantin, F., Génard, M., Turc, O., Freixes, S., Piques, M. and Gibon, Y.: Water deficits
881 uncouple growth from photosynthesis, increase C content, and modify the relationships between
882 C and growth in sink organs., *J. Exp. Bot.*, 62(6), 1715–29, doi:10.1093/jxb/erq438, 2011.
- 883 Mund, M., Kutsch, W. L., Wirth, C., Kahl, T., Knohl, a, Skomarkova, M. V and Schulze, E.-D.:
884 The influence of climate and fructification on the inter-annual variability of stem growth and net
885 primary productivity in an old-growth, mixed beech forest., *Tree Physiol.*, 30(6), 689–704,
886 doi:10.1093/treephys/tpq027, 2010.
- 887 Ohtsuka, T., Saigusa, N. and Koizumi, H.: On linking multiyear biometric measurements of tree
888 growth with eddy covariance-based net ecosystem production, *Glob. Chang. Biol.*, 15(4), 1015–
889 1024, 2009.
- 890 Palacio, S., Hernández, R., Maestro-Martínez, M. and Camarero, J. J.: Fast replenishment of
891 initial carbon stores after defoliation by the pine processionary moth and its relationship to the
892 re-growth ability of trees, *Trees*, 26(5), 1627–1640, 2012.
- 893 Palacio, S., Hoch, G., Sala, A., Körner, C. and Millard, P.: Does carbon storage limit tree
894 growth?, *New Phytol.*, 201(4), 1096–1100, doi:10.1111/nph.12602, 2014.
- 895 Pan, Y., Birdsey, R. a, Fang, J., Houghton, R., Kauppi, P. E., Kurz, W. a, Phillips, O. L.,
896 Shvidenko, A., Lewis, S. L., Canadell, J. G., Ciais, P., Jackson, R. B., Pacala, S. W., McGuire, a
897 D., Piao, S., Rautiainen, A., Sitch, S. and Hayes, D.: A large and persistent carbon sink in the
898 world's forests., *Science*, 333(6045), 988–93, doi:10.1126/science.1201609, 2011.
- 899 Pasquet, K.: Determiation des chuttes de litières sur le réseau RENECOFOR de 1995 à 2002,
900 Off. Natl. des forêts, Département des Rech. Tech., 2002.
- 901 Peichl, M., Brodeur, J. J., Khomik, M. and Arain, M. A.: Biometric and eddy-covariance based
902 estimates of carbon fluxes in an age-sequence of temperate pine forests, *Agric. For. Meteorol.*,
903 150(7-8), 952–965, doi:10.1016/j.agrformet.2010.03.002, 2010.
- 904 Ponette, Q.: Chimie des sols dans les 102 peuplements du réseau, Office National des Forêts-
905 Direction Technique., 1997.

- 906 Rambal, S., Joffre, R., Ourcival, J. M., Cavender-Bares, J. and Rocheteau, A.: The growth
907 respiration component in eddy CO₂ flux from a *Quercus ilex* mediterranean forest, *Glob. Chang.*
908 *Biol.*, 10(9), 1460–1469, 2004.
- 909 Richardson, A. D., Carbone, M. S., Keenan, T. F., Czimczik, C. I., Hollinger, D. Y., Murakami, P.,
910 Schaberg, P. G. and Xu, X.: Seasonal dynamics and age of stemwood nonstructural
911 carbohydrates in temperate forest trees, *New Phytol.*, 197(3), 850–861, 2013.
- 912 Rocha, A. V., Goulden, M. L., Dunn, A. L. and Wofsy, S. C.: On linking interannual tree ring
913 variability with observations of whole-forest CO₂ flux, *Glob. Chang. Biol.*, 12(8), 1378–1389,
914 doi:10.1111/j.1365-2486.2006.01179.x, 2006.
- 915 Rossi, S., Anfodillo, T., Cufar, K., Cuny, H. E., Deslauriers, A., Fonti, P., Frank, D., Gricar, J.,
916 Gruber, A., King, G. M., Krause, C., Morin, H., Oberhuber, W., Prislán, P. and Rathgeber, C. B.
917 K.: A meta-analysis of cambium phenology and growth: linear and non-linear patterns in conifers
918 of the northern hemisphere., *Ann. Bot.*, 112(9), 1911–20, doi:10.1093/aob/mct243, 2013.
- 919 Rossi, S., Morin, H., Deslauriers, A. and Plourde, P.-Y.: Predicting xylem phenology in black
920 spruce under climate warming, *Glob. Chang. Biol.*, 17(1), 614–625, 2011.
- 921 Ryan, M. G., Phillips, N. and Bond, B. J.: The hydraulic limitation hypothesis revisited, *Plant Cell*
922 *Environ.*, 29(3), 367–81, doi:10.1111/j.1365-3040.2005.01478.x, 2006.
- 923 Sala, A., Woodruff, D. R. and Meinzer, F. C.: Carbon dynamics in trees: feast or famine?, *Tree*
924 *Physiol.*, 32(6), 1–12, doi:10.1093/treephys/tpr143, 2012.
- 925 Schiestl-Aalto, P., Kulmala, L., Mäkinen, H., Nikinmaa, E. and Mäkelä, A.: CASSIA—a dynamic
926 model for predicting intra-annual sink demand and interannual growth variation in Scots pine,
927 *New Phytol.*, doi:10.1111/nph.13275, 2015.
- 928 Seynave, I., Gégout, J., Hervé, J., Drapier, J., Bruno, É. and Dumé, G.: *Picea abies* site index
929 prediction by environmental factors and understorey vegetation : a two-scale approach based on
930 survey databases, , 1678, 1669–1678, doi:10.1139/X05-088, 2005.
- 931 Sitch, S., Smith, B., Prentice, I. C., Arneth, A., Bondeau, A., Cramer, W., Kaplan, J. O., Levis, S.,
932 Lucht, W. and Sykes, M. T.: Evaluation of ecosystem dynamics, plant geography and terrestrial
933 carbon cycling in the LPJ dynamic global vegetation model, *Glob. Chang. Biol.*, 9(2), 161–185,
934 2003.
- 935 Tang, J., Luysaert, S., Richardson, A. D., Kutsch, W. and Janssens, I. A.: Steeper declines in
936 forest photosynthesis than respiration explain age-driven decreases in forest growth, *Proc. Natl.*
937 *Acad. Sci.*, doi: 10.1073/pnas.1320761111, 2014.
- 938 Tardieu, F., Granier, C. and Muller, B.: Water deficit and growth. Co-ordinating processes
939 without an orchestrator?, *Curr. Opin. Plant Biol.*, 14(3), 283–289, 2011.
- 940 Thomas, S. C.: Age-related changes in tree growth and functional biology: the role of
941 reproduction, in *Size-and age-related changes in tree structure and function*, pp. 33–64,
942 Springer., 2011.

- 943 Ulrich, E.: Organization of forest system monitoring in France-the RENECOFOR network, in
944 World Forestry Congress, Antalya, TR., 1997.
- 945 Vallet, P., Dhôte, J.-F., Moguédec, G. Le, Ravart, M. and Pignard, G.: Development of total
946 aboveground volume equations for seven important forest tree species in France, *For. Ecol.*
947 *Manage.*, 229(1-3), 98–110, doi:10.1016/j.foreco.2006.03.013, 2006.
- 948 Vicca, S., Luysaert, S., Peñuelas, J., Campioli, M., Chapin, F. S., Ciais, P., Heinemeyer, a,
949 Högberg, P., Kutsch, W. L., Law, B. E., Malhi, Y., Papale, D., Piao, S. L., Reichstein, M.,
950 Schulze, E. D. and Janssens, I. a: Fertile forests produce biomass more efficiently., *Ecol. Lett.*,
951 15(6), 520–6, doi:10.1111/j.1461-0248.2012.01775.x, 2012.
- 952 Vidal, J.-P., Martin, E., Franchistéguy, L., Baillon, M. and Soubeyroux, J.-M.: A 50-year high-
953 resolution atmospheric reanalysis over France with the Safran system, *Int. J. Climatol.*, 30(11),
954 1627–1644, doi:10.1002/joc.2003, 2010.
- 955 Vitasse, Y., Lenz, A., Kollas, C., Randin, C. F., Hoch, G. and Körner, C.: Genetic vs. non-genetic
956 responses of leaf morphology and growth to elevation in temperate tree species, *Funct. Ecol.*,
957 28(1), 243–252, 2014.
- 958 Wiley, E. and Helliker, B.: A re-evaluation of carbon storage in trees lends greater support for
959 carbon limitation to growth, *New Phytol.*, 195(2), 285–289, 2012.
- 960 Wiley, E., Huepenbecker, S., Casper, B. B. and Helliker, B. R.: The effects of defoliation on
961 carbon allocation: can carbon limitation reduce growth in favour of storage?, *Tree Physiol.*,
962 33(11), 1216–1228, 2013.
- 963 Wilhelmsson, L., Arlinger, J., Spångberg, K., Lundqvist, S.-O., Grahn, T., Hedenberg, Ö. and
964 Olsson, L.: Models for Predicting Wood Properties in Stems of *Picea abies* and *Pinus sylvestris*
965 in Sweden, *Scand. J. For. Res.*, 17(4), 330–350, doi:10.1080/02827580260138080, 2002.
- 966 Wolf, A., Field, C. B. and Berry, J. A.: Allometric growth and allocation in forests: a perspective
967 from FLUXNET, *Ecol. Appl.*, 21(5), 1546–1556, 2011.
- 968 Woodruff, D. R., Bond, B. J. and Meinzer, F. C.: Does turgor limit growth in tall trees?, *Plant. Cell*
969 *Environ.*, 27(2), 229–236, 2004.
- 970 Woodruff, D. R. and Meinzer, F. C.: Size-dependent changes in biophysical control of tree
971 growth: the role of turgor, in *Size-and age-related changes in tree structure and function*, pp.
972 363–384, Springer., 2011.
- 973 Würth, M. K. R., Peláez-Riedl, S., Wright, S. J. and Körner, C.: Non-structural carbohydrate
974 pools in a tropical forest., *Oecologia*, 143(1), 11–24, doi:10.1007/s00442-004-1773-2, 2005.
- 975 Xu, C., Turnbull, M. H., Tissue, D. T., Lewis, J. D., Carson, R., Schuster, W. S. F., Whitehead,
976 D., Walcroft, A. S., Li, J. and Griffin, K. L.: Age-related decline of stand biomass accumulation is
977 primarily due to mortality and not to reduction in NPP associated with individual tree physiology,
978 tree growth or stand structure in a *Quercus*-dominated forest, *J. Ecol.*, 100(2), 428–440, 2012.

- 979 Zha, T. S., Barr, a. G., Bernier, P.-Y., Lavigne, M. B., Trofymow, J. a., Amiro, B. D., Arain, M. a.,
980 Bhatti, J. S., Black, T. a., Margolis, H. a., McCaughey, J. H., Xing, Z. S., Van Rees, K. C. J. and
981 Coursolle, C.: Gross and aboveground net primary production at Canadian forest carbon flux
982 sites, *Agric. For. Meteorol.*, 174-175, 54–64, doi:10.1016/j.agrformet.2013.02.004, 2013.
- 983 Zhang, S.-Y., Owoundi, R. E., Nepveu, G., Mothe, F. and Dhôte, J.-F.: Modelling wood density in
984 European oak (*Quercuspetraea* and *Quercusrobur*) and simulating the silvicultural influence,
985 *Can. J. For. Res.*, 23(12), 2587–2593, doi:10.1139/x93-320, 1993.
- 986 Zweifel, R., Eugster, W., Etzold, S., Dobbertin, M., Buchmann, N. and Häsler, R.: Link between
987 continuous stem radius changes and net ecosystem productivity of a subalpine Norway spruce
988 forest in the Swiss Alps, *New Phytol.*, 187(3), 819–830, 2010.
- 989 Zweifel, R., Zimmermann, L., Zeugin, F. and Newbery, D. M.: Intra-annual radial growth and
990 water relations of trees: implications towards a growth mechanism., *J. Exp. Bot.*, 57(6), 1445–59,
991 doi:10.1093/jxb/erj125, 2006.
- 992

Table 1. Climate of the study sites. ETP: annual Penman - Monteith potential evapotranspiration; Precip.: annual precipitation; Temp.: annual temperature. Values are site averages \pm standard deviation among sites.

Species	number of plots	number of site-years	elevation (m)	ETP (mm)	Precip. (mm)	Temp. (°C)	Source
<i>F. sylvatica</i>	16	313	565 \pm 326	1010 \pm 121	1001 \pm 133	10.1 \pm 0.98	RENECOFOR
<i>Q. petraea</i> / <i>Q. robur</i>	26	484	193 \pm 76	999 \pm 71	821 \pm 96	10.7 \pm 0.63	RENECOFOR
<i>P. abies</i>	6	101	1056 \pm 313	933 \pm 44	1559 \pm 340	7.1 \pm 1.4	RENECOFOR
<i>Q. ilex</i>	1	43	270	1417	907	13.4	Puéchabon site

Table 2. Description of explanatory variables. The “Type” category indicates the source of the data: field measurement (M), SAFRAN climate database (C) or CASTANEA simulation (S). The “Scale” categories indicate whether the variable was considered in the spatial (S) and temporal (T) analyses.

IDs	Description	Unit	Type	Scale
<i>age</i>	Stand age	years	M	S
<i>AWBI</i>	Annual woody biomass increment	gC.m ⁻²	M	ST
<i>SBA</i>	Stand basal area	m ²	M	S
<i>camb_onset</i>	Onset of the cambial activity	day of the year	S	T
<i>GPP_{gp}</i>	Gross primary production of the current (y) growth period	gC.m ⁻²	S	ST
<i>GPP_{y-1}</i>	Gross primary production of the previous (y-1) year	gC.m ⁻²	S	T
<i>frost</i>	Sum of the average daily temperatures below -2°C during the last winter (year y-1 and y)	°C	C	ST
<i>LNC</i>	Leaf nitrogen content	gN.gDM ⁻¹	M	S
<i>NPP_{gp}</i>	Net primary production of the current (y) growth period	gC.m ⁻²	S	ST
<i>NPP_{y-1}</i>	Net primary production of the previous (y-1) year	gC.m ⁻²	S	T
<i>numstem</i>	Stem density	number.ha ⁻¹	M	S
<i>SNA</i>	Class of soil nutrient availability (1: low, 2: medium, 3: high)	unitless	M	S
<i>SWHC</i>	Soil water holding capacity	mm	M	S
<i>templim_{gp}</i>	Number of days of the current (y) growth period with an average temperature below 6°C	number of days	C	ST
<i>Ra_{gp}</i>	Autotrophic respiration of the current (y) growth period	gC.m ⁻²	S	ST
<i>Ra_{y-1}</i>	Autotrophic respiration of the previous (y-1) year	gC.m ⁻²	S	T
<i>WS_{per_{gp}}</i>	Number of days of the current (y) growth period with soil water content below 60% of the soil water holding capacity	number of days	S	ST
<i>WS_{per_{y-1}}</i>	Number of days of the previous (y-1) year with soil water content below 60% of the soil water holding capacity	number of days	S	T
<i>WS_{int_{gp}}</i>	Water stress intensity index over the current (y) growth period	unitless	S	ST
<i>WS_{int_{y-1}}</i>	Water stress intensity index of the previous (y-1) year	unitless	S	T

Table 3. Relationships of annual wood growth and the components of the seasonal forest carbon balance: NPP, GPP and Ra. The *start* and *end* terms (day of the year) indicate the carbon flux period that yielded the maximum value for the median of the growth-flux correlations among sites. The *r* term is the maximum obtained for the median of the site-specific Pearson correlation coefficients; values that are significantly different from 0 are indicated (* indicates $P < 0.05$ and ** indicates $P < 0.001$). The σ term is the standard deviation of the Pearson correlation values among sites.

Species	GPP				Ra				NPP			
	<i>start</i>	<i>end</i>	<i>r</i>	σ	<i>start</i>	<i>end</i>	<i>r</i>	σ	<i>start</i>	<i>end</i>	<i>r</i>	σ
<i>F. sylvatica</i>	124	258	0.62**	0.18	96	200	-0.29*	0.33	126	262	0.58**	0.24
<i>Q. petraea</i> / <i>Q. robur</i>	136	214	0.59**	0.25	98	192	0.31*	0.24	130	214	0.50**	0.28
<i>P. abies</i>	32	262	0.52**	0.38	78	348	0.11	0.52	32	200	0.49**	0.29
<i>Q. ilex</i>	186	226	0.60		36	256	-0.26		186	226	0.58	

Table 4. Spatial dependences of annual wood growth: multiple regression estimates. The data have been centred and scaled. GPP_{gp} is the GPP of the growth period, age is the average age of the stand, and SBA is the stand basal area (Table 2). Values: estimates [F values]. All estimated values differed significantly from 0 ($P < 0.001$). All variables were retained in the bootstrap procedure (see main text).

Species	Estimates			P	adj. R ²
	GPP_{gp}	age	SBA		
<i>Q. petraea</i> / <i>Q. robur</i>		-8.88×10^{-1} [39.5]	4.27×10^{-1} [19.5]	$<10^{-4}$	0.69
<i>F. sylvatica</i>	5.07×10^{-1} [59.4]	-6.96×10^{-1} [61.6]		$<10^{-4}$	0.88
<i>P. abies</i>	8.25×10^{-1} [8.6]			0.04	0.60

Table 5. Temporal dependences of annual wood growth: multiple regression estimates. The data have been centred and scaled. GPP_{gp} is the GPP of the growth period, $WS_{per_{gp}}$ is the water stress index of the growth period, $WS_{int_{y-1}}$ is the water stress index of the previous year, and $templim_{gp}$ is the low temperature index of the growth period (see Table 2). D1 and D2 are dummy variables (D1 = 0 if $GPP_{gp} < 1400 \text{ gC m}^{-2}$; otherwise, D1 = 1. D2 = 0 if $GPP_{y-1} < 1550 \text{ gC m}^{-2}$; otherwise, D2 = 1; see Fig. 5). The ρ term is the parameter of the first-order autoregressive process that was used to model the temporal autocorrelation of the within-stand errors. Values: estimates [F values]. Estimated values that are significantly different from 0 are indicated (* indicates $P < 0.05$, ** indicates $P < 0.01$, and *** indicates $P < 0.001$). A Δ index indicates that the variable was not retained in the bootstrap procedure (see main text).

Estimates	Species			
	<i>Q. petraea</i> / <i>Q. robur</i>	<i>F. sylvatica</i>	<i>P. abies</i>	<i>Q. ilex</i>
GPP_{gp}	3.26×10^{-1} ***	4.87×10^{-1} ***	2.4×10^{-1} * [3.5]	
$WS_{per_{gp}}$	-1.09×10^{-1} **	-2.04×10^{-1} ***		-5.8×10^{-1} ***
$WS_{int_{y-1}}$		-2.37×10^{-1} ***		-2.2×10^{-1} * [6.3]
GPP_{y-1}	3.82×10^{-1} * [3.3]		-4×10^{-1} ** [3.2]	
$templim_{gp}$	-9.60×10^{-2} ** Δ		-1.26 *** [3.5]	
D1			-2.4×10^{-1} ***	
D2	-3.9×10^{-1} ** [0.8]			
D1 * GPP_{gp}			1.33 ** [8.2]	
D2 * GPP_{y-1}	-4×10^{-1} ** [6.4]			
ρ	0.61	0.68	0.52	0.44
P	$<10^{-4}$	$<10^{-4}$	$7.7 \cdot 10^{-3}$	$<10^{-4}$
adj. R²	0.21	0.42	0.20	0.43

Figure captions

Figure 1. **The conceptual framework and the three sources of data (field measurements, climate reanalysis, and process-based simulations) used in the analyses.**

Figure 2. **Locations of the study sites.**

Figure 3. **Spatial dependences of annual wood growth.** A: Relationship of the AWBI and the GPP of the growth period (GPP_{gp}) averaged over sites. B: Age-related decline of the C partitioning to AWBI ($AWBI / GPP_{gp}$).

Figure 4. **Temporal dependences of annual wood growth: the roles of explanatory variables from RF classification.** Variable importance is expressed as the percentage of the importance of the top-ranked explanatory variable. The variable identifiers (IDs) are listed in Table 2. The coloured variables were retained in subsequent analyses.

Figure 5. **Temporal dependences of annual wood growth: marginal effects of each explanatory variable on the annual wood growth.** The lines represent smoothing splines with 50% frequency response cut-offs. The coloured areas indicate the 95% confidence intervals. The 5% and 95% data quantiles (grey areas) were not considered in the discussion. The marginal effect of a given variable X was obtained by fixing the value of X and averaging the RF predictions over all the combinations of observed values for the other predictors in the dataset (Cutler et al., 2007). The marginal predictions were collected over the entire range of X in the training data using a regular grid.

Figure 6. **Modelling framework for a combined source- and sink-driven representation of C allocation to wood growth.**

Figure 1.

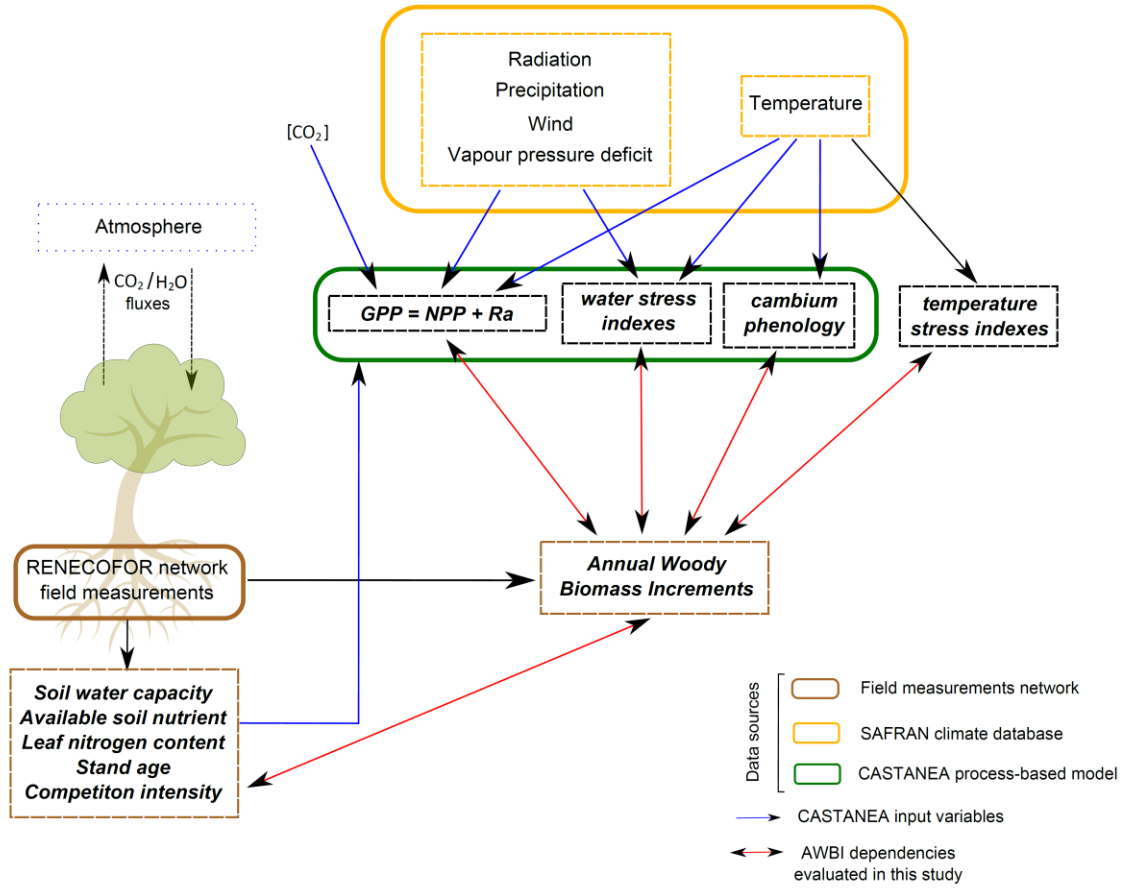


Figure 2.

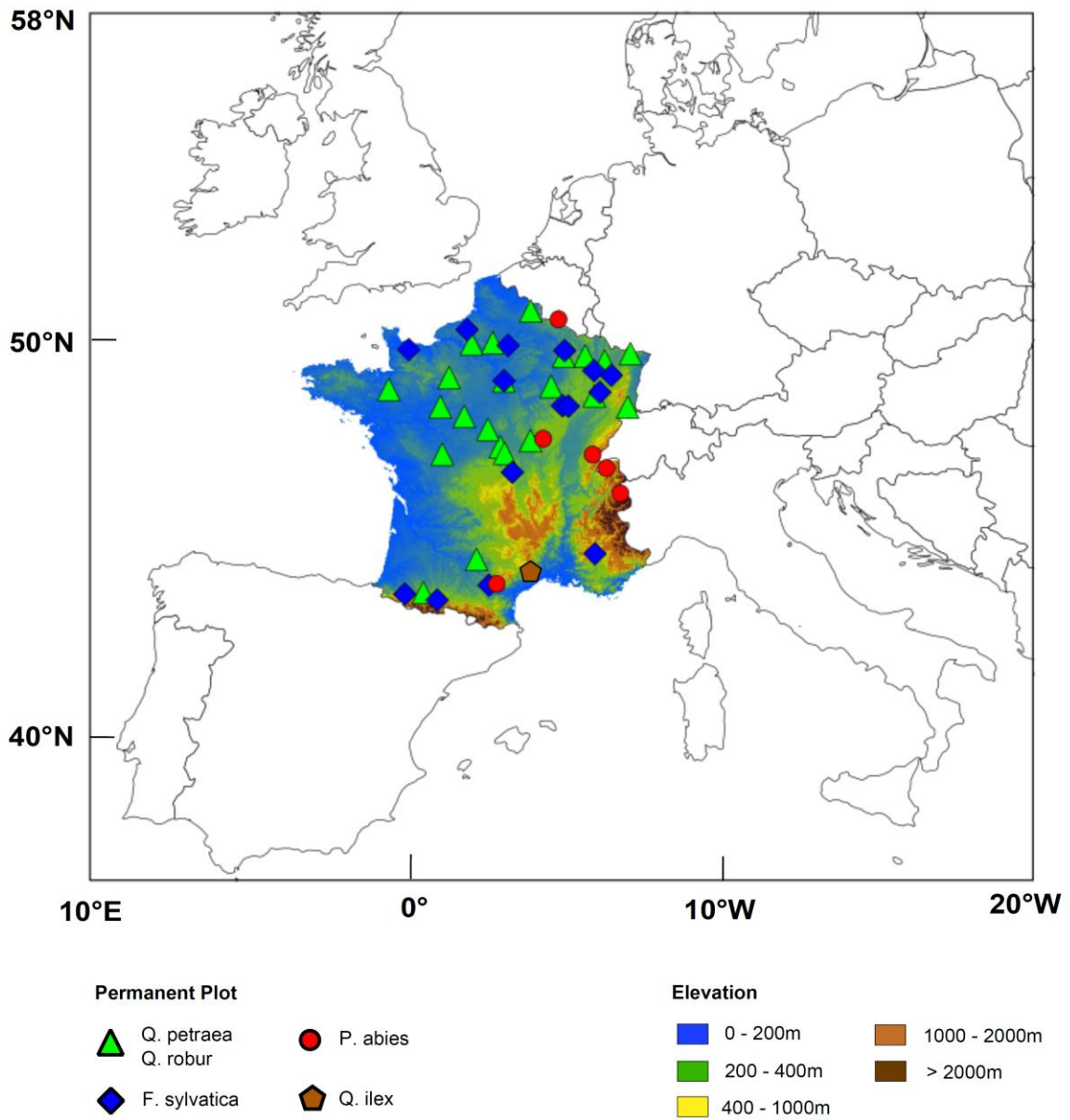


Figure 3.

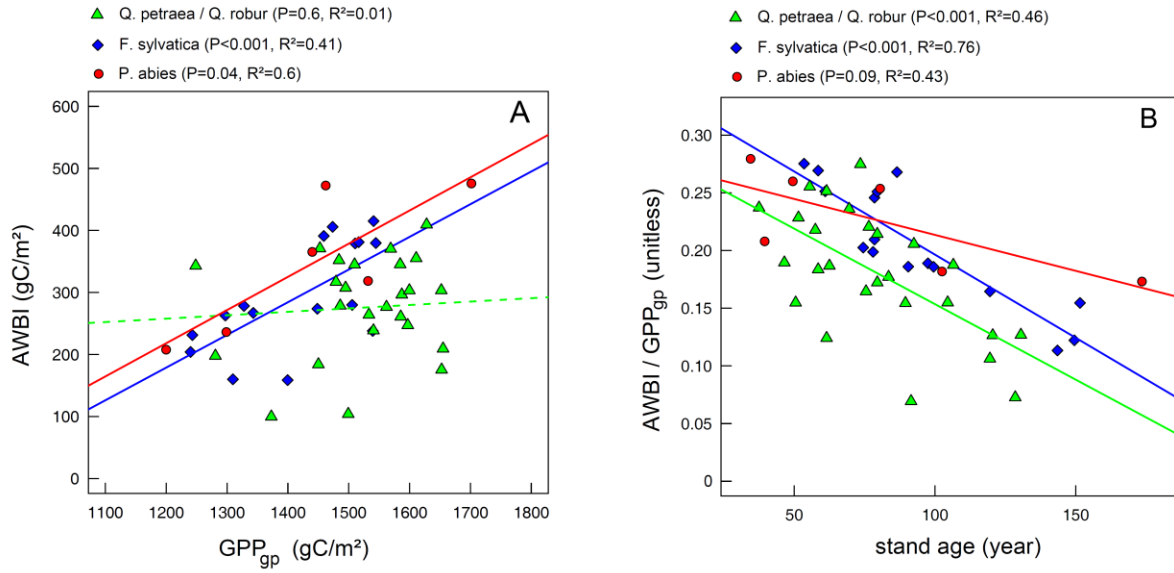


Figure 4.

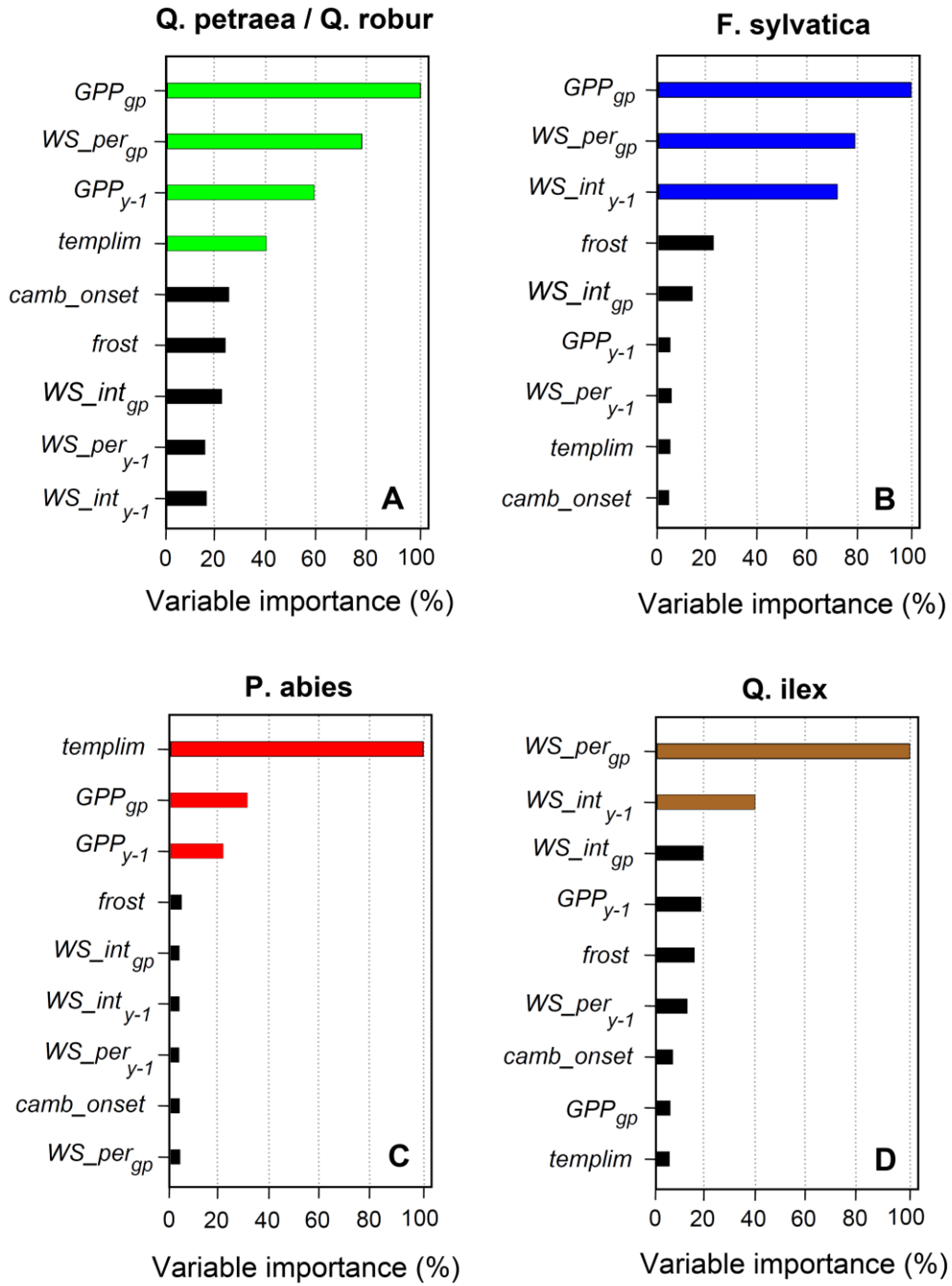


Figure 5.

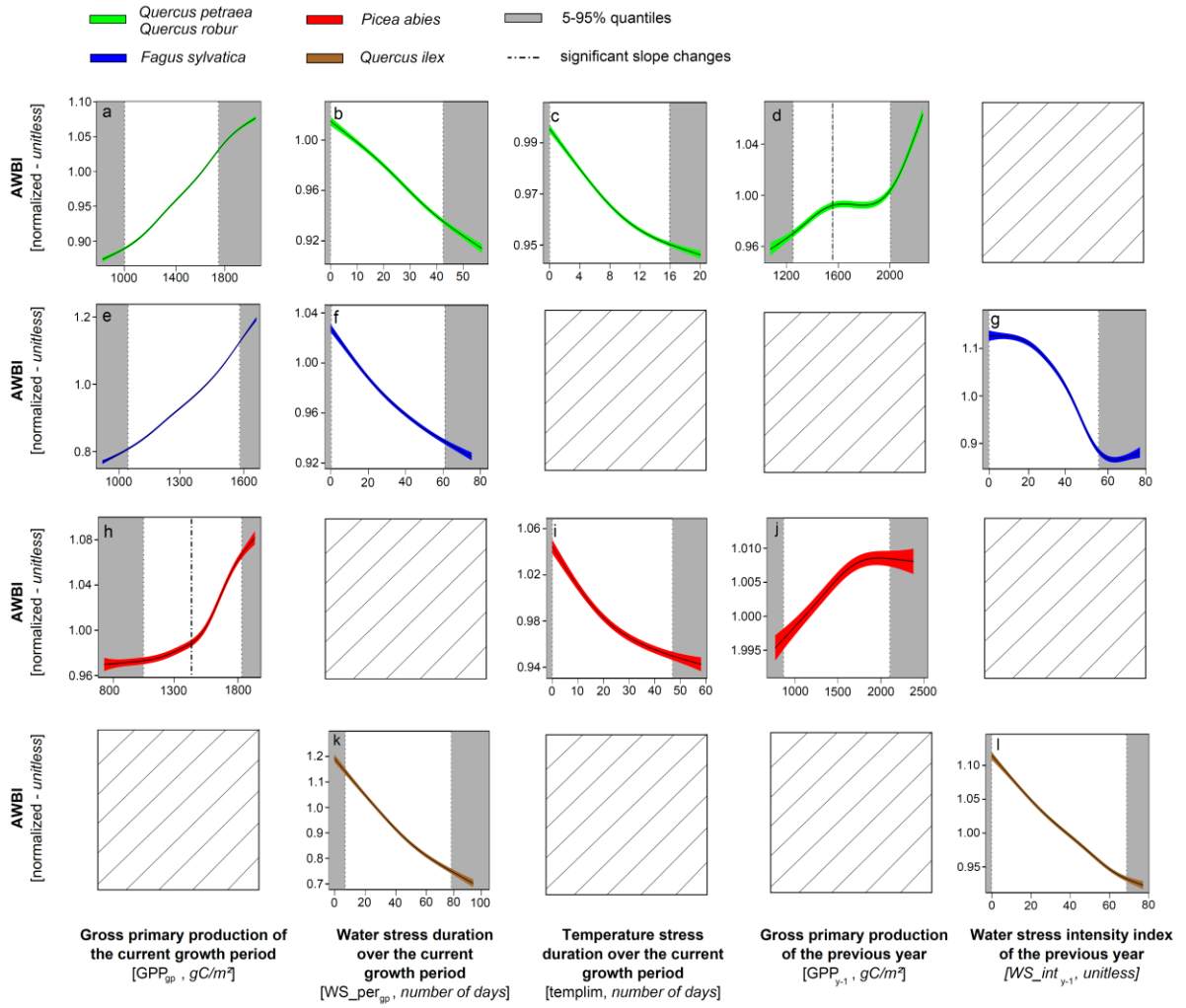


Figure 6.

